In vivo tracking of phosphoinositides in *Drosophila* photoreceptors

[1]Roger C Hardie, [1]Che-Hsiung Liu, [1]Alexander S Randall, [1,2]Sukanya Sengupta

[1]Department of Physiology Development and Neuroscience, Cambridge University CB2 3EG United Kingdom

[2]Present address Tufts Center for Neuroscience Research, Tufts University School of Medicine, 136 Harrison Avenue, Boston MA 02111 U.S.A.

Corresponding author: Roger Hardie rch14@cam.ac.uk

Key words PIP_2, pleckstrin homology domain, phototransduction, fluorescent probes, GFP, voltage-sensitive phosphatase

JCS Advance Online Article. Posted on 19 October 2015

Abstract

In order to monitor phosphoinositide turnover during phospholipase C (PLC) mediated *Drosophila* phototransduction, fluorescently tagged lipid probes were expressed in photoreceptors and imaged both in dissociated cells, and in eyes of intact living flies. Of six probes tested, Tb^{R332H} (mutant of the Tubby protein pleckstrin homology domain) was judged the best reporter for PtdIns(4,5)P_2, and the P4M domain from *Legionella* SidM for PtdIns4*P*. Using accurately calibrated illumination, these indicated that only ~50% of PtdIns(4,5)P_2 and very little PtdIns4*P* were depleted by full daylight intensities in wild-type flies, but both were severely depleted by ~100-fold dimmer intensities in mutants lacking Ca^{2+} permeable TRP channels or protein kinase C (PKC). Resynthesis of PtdIns4*P* (t½ ~12 s) was faster than PtdIns(4,5)P_2 (t½ ~40s), but both were greatly slowed in mutants of DAG kinase (*rdgA*) or PtdIns transfer protein (*rdgB*). The results indicate that Ca^{2+} and PKC-dependent inhibition of PLC is critical for enabling photoreceptors to maintain phosphoinositide levels despite high rates of hydrolysis by PLC, and suggest phosphorylation of PtdIns4*P* to PtdIns(4,5)P_2 is the rate-limiting step of the cycle.

Introduction

Phototransduction in *Drosophila* is mediated by a G-protein coupled phospholipase C (PLC) cascade and is an influential model for phosphoinositide signalling (Hardie, 2012; Hardie and Juusola, 2015; Katz and Minke, 2009; Montell, 2012; Yau and Hardie, 2009). The electrical response to light is mediated by two Ca^{2+} permeable cation channels: "transient receptor potential" (TRP) - and TRP-like (TRPL) (Hardie and Minke, 1992; Montell and Rubin, 1989; Phillips et al., 1992). Like their mammalian TRPC homologues, both are activated downstream of PLC. The channels are localised in a light-guiding "rhabdomere" (a rod-like stack of ~30000 microvilli) along with other components of the phototransduction cascade, including rhodopsin, Gq protein and PLCβ4 (Hardie, 2012; Huber et al., 1996). How hydrolysis of PtdIns(4,5)P_2 by PLC activates TRP and TRPL remains debated. Recent evidence has suggested a combinatorial mechanism requiring both a reduction in PtdIns(4,5)P_2 and acidification mediated by the protons released by the PLC reaction (Huang et al., 2010). The depletion of PtdIns(4,5)P_2 may act mechanically by cleaving its large and highly charged headgroup from the membrane, leading to a physical contraction of the microvillar membrane (Hardie and Franze, 2012).

PtdIns(4,5)P_2 and other phosphoinositides are vital regulators of numerous cellular functions (Balla, 2013; Di Paolo and De Camilli, 2006; Hilgemann et al., 2001; Payrastre et al., 2001; Rohacs, 2009; Yin and Janmey, 2003), hence their metabolism plays critical roles in many cells. Previous studies indicated that light-induced PtdIns(4,5)P_2 hydrolysis by PLC in *Drosophila* is initially very rapid, but then abruptly inhibited by Ca^{2+} influx via the TRP channels (Gu et al., 2005; Hardie et al., 2004; Hardie et al., 2001). In these experiments, PtdIns(4,5)P_2 was monitored using a genetically encoded electrophysiological biosensor - the Kir2.1 potassium channel, which is activated by PtdIns(4,5)P_2 (Hilgemann and Ball, 1996). Although a powerful tool, Kir2.1's use as a biosensor necessitates patch-clamp recordings, which are invasive, technically demanding and have a limited lifetime. Another class of tools used to monitor phosphoinositide turnover, are fluorescently tagged phosphoinositide binding domains. The first and most widely used of these was the pleckstrin homology (PH) domain from PLCδ1 (Stauffer et al., 1998; Varnai and Balla, 1998). However, interpretation is complicated because PLCδ1-PH binds Ins(1,4,5)P_3 as well

as PtdIns(4,5)P_2 (e.g. Hirose et al., 1999; Nash et al., 2001; Szentpetery et al., 2009). More recently, PtdIns(4,5)P_2 probes with negligible affinity for $InsP_3$, based on the Tubby protein were developed (Hughes et al., 2007; Quinn et al., 2008), whilst probes with affinity for other phosphoinositide species are also available (Balla et al., 2009; Balla and Varnai, 2009; Szentpetery et al., 2009; Yu et al., 2004).

In the present study we expressed a range of fluorescently tagged lipid probes in *Drosophila* photoreceptors. We used them to monitor phosphoinositide turnover, both in dissociated cells and in intact flies by exploiting the optics of the compound eye, which allow imaging of the rhabdomeres in live animals over many hours. Combined with the ability to activate the cascade with precisely calibrated illumination, and expression of a voltage-sensitive phosphatase allowing depletion of PtdIns(4,5)P_2 by conversion to PtdIns4*P* (Iwasaki et al., 2008; Murata et al., 2005), we used these probes to provide quantitative insight into phosphoinositide turnover under physiologically relevant illumination in both wild-type flies and a variety of mutant backgrounds.

Results

A range of fluorescently tagged lipid binding domains were expressed in *Drosophila* photoreceptors under control of the rhodopsin (*ninaE* = Rh1) or *trp* promoters. These included GFP-tagged PLCδ1 PH (subsequently referred to as PH-GFP), which binds to both PtdIns(4,5)P_2 and Ins(1,4,5)P_3 (Hirose et al., 1999; Stauffer et al., 1998; Szentpetery et al., 2009; Varnai and Balla, 1998); a PH domain from the C-terminal of the Tubby protein (YFP-tagged), which has a high affinity for PtdIns(4,5)P_2 but negligible affinity for Ins(1,4,5)P_3 (Santagata et al., 2001); a point mutation of the same construct, Tb^{R332H}, with reduced affinity for PtdIns(4,5)P_2 (Quinn et al., 2008); OSH2 (GFP-tagged), which binds both PtdIns4*P* and PtdIns(4,5)P_2 with similar affinities; OSH1(GFP-tagged) which also binds PtdIns4*P* and PtdIns(4,5)P_2 – but with ~3-fold lower affinity than OSH2 (Yu et al., 2004), and the P4M domain (GFP-tagged) of *Legionella* SidM, which binds to PtdIns4*P* but not PtdIns(4,5)P_2 (Brombacher et al., 2009; Hammond et al., 2014). In preliminary experiments the wild-type Tubby PH domain translocated much more sluggishly than the other probes, suggesting its affinity was too high to be a useful indicator of PtdIns(4,5)P_2 turnover in the photoreceptors, and it was not used further.

In principle, expression of PtdIns(4,5)P_2 binding proteins in the microvilli might affect phototransduction, for example by sequestering PtdIns(4,5)P_2. However, light responses in whole-cell patch clamp recordings from photoreceptors expressing the probes showed no significant differences from wild-type photoreceptors, with normal response kinetics, absolute sensitivity and single photon responses (Fig. S1). Morphology at the light-microscope level was also not noticeably affected (e.g. Fig. 1) and cell capacitances, which provide a measure of the area of microvillar membrane, were indistinguishable from wild type (Fig. S1).

To visualise the subcellular localization of the probes, dissociated ommatidia were imaged with conventional epi-fluorescence microscopy. Because the blue excitation light is a saturating stimulus for the photoreceptors, only the first image frame represents the dark-adapted situation, and any subsequent dynamic redistribution reflects the response to the blue excitation. In dark-adapted photoreceptors, all probes were initially well localized to the microvillar rhabdomeres, visible as brightly fluorescing rod-like tracks towards the centre of the ommatidia (Fig. 1). With little

delay, fluorescence rapidly decreased in the rhabdomeres, and increased in cell body regions, reflecting translocation of the probes as PtdIns(4,5)P_2 and/or PtdIns4*P* was depleted by light-activated PLC (Movies S1-S3). The different probes translocated with subtly different patterns: PH-GFP accumulated diffusely in the cytosol, whilst Tb^{R332H} accumulated mainly on non-microvillar plasma membrane. OSH2, OSH1 and P4M also accumulated in discrete regions within the cell presumably representing intracellular membranes (e.g Golgi/endosome) as well as some mobile vesicles. These patterns are consistent with the reported affinities of the different probes. Thus only PH-GFP also binds to Ins(1,4,5)P_3, ($InsP_3$), which would be expected to diffuse freely into the cytosolic aqueous phase. Tb^{R332H} binds specifically to PtdIns(4,5)P_2 , which is expected to have a predominantly plasma membrane localization. OSH1, OSH2 and P4M bind to PtdIns4*P*, which has been localized to Golgi, plasma membrane and motile vesicles in mammalian cells (Hammond et al., 2014).

To quantify the signals, intensity was measured in regions of interest (ROI) in the rhabdomere and the cytosol (Fig. 1), and the relative rhabdomere fluorescence ($F_{rh/cyt}$) plotted as a function of time. $F_{rh/cyt}$ decayed with time constants of ~7s for Tb^{R332H}, ~10-15 s for P4M, OSH2 and OSH1. PH-GFP translocated remarkably rapidly with a time constant of ~1 s (Fig. 1C). In terms of extent of translocation, Tb^{R332H} showed the greatest reduction in $F_{rh/cyt}$ (~2.5 fold), with OSH2, P4M and PH-GFP all showing ~2-fold reduction. Although robust, the OSH1 signal showed only relatively minor (1.3 fold) reduction and was not used systematically for further experiments (Fig. 1D).

A complication inherent in any fluorescent study involving photoreceptors is that the excitation light itself is usually a supersaturating stimulus, photoisomerizing a large fraction of the visual pigment rhodopsin (R) to its active metarhodopsin (M) state . In microvillar opsins such as those in *Drosophila*, the two states (R and M) are thermostable and photo-interconvertible, and therefore exist in a photoequilibrium determined by their absorption spectra and the spectral content of illumination (Minke and Kirschfeld, 1979). Since R absorbs maximally at 480 nm and M at 570 nm, the blue excitation light preferentially converts R to M, creating a photoequilibrium with ~70% M / 30% R, which is reached within less than 100 ms (see Fig. S4) and then maintained indefinitely (many hours), or until M is photo-reisomerized to R by

absorption of long wavelength light. The active M state continues to activate the cascade (via G-proteins) until it is inactivated by binding to arrestin. However, because arrestin molecules are in limited supply (~ 1/3 of the number of visual pigment molecules), there are insufficient to bind to and inactivate this amount (70%) of M. This results in maintained saturating activation of the phototransduction cascade and a so-called prolonged depolarizing afterpotential (PDA), which lasts for many hours (Dolph et al., 1993; Minke, 1979). Apparently, in this PDA state, PtdIns(4,5)P_2 and PtdIns4P in the rhabdomeres are largely depleted and remain so indefinitely, because even after prolonged periods in the dark, there was little if any recovery of fluorescence in the rhabdomeres by any of the probes either in dissociated ommatidia or in intact animals using the deep pseudopupil (see below and Fig. 4B). However, if M was photoreisomerised to the rhodopsin (R) state by long wavelength (640 nm LED) light, substantial fractions of all probes returned to the rhabdomeres within 1 or 2 minutes in the dark, indicating resynthesis of PtdIns4P and PtdIns(4,5)P_2 (see further below).

Deep pseudopupil measurements

Although fluorescent probes can be tracked with high resolution in dissociated ommatidia, this preparation is relatively short-lived (~2 hrs) and vulnerable to damage by the intense illumination required to excite fluorescence. In order to obtain more quantitative data under physiological conditions, we exploited the optics of the compound eye to image fluorescence in the rhabdomeres in intact flies. As described in classic studies from the 1970's (e.g. Franceschini and Kirschfeld, 1971), by focussing a low power objective below the surface of the eye where the optical axes of neighbouring ommatidia converge, the characteristic rhabdomere pattern is seen as a magnified virtual image known as the deep pseudopupil (DPP). Not only does this collect light from many tens of ommatidia, but because of their wave-guiding properties, the rhabdomeres' fluorescence is directional and channelled to the objective, whilst fluorescence from the cell body is diffuse and comparatively weak (Fig. 2A). Fluorescence measured from the DPP thus provides a measure of the concentration of the probe in the rhabdomere. This non-invasive preparation is very robust, allowing repeated measurements over many hours, and provides a rare opportunity for live tracking of fluorescent probes in a subcellular compartment in completely intact animals (Meyer et al., 2006; Satoh et al., 2010).

Figure 2 shows frames from movies (Movies S4-5) of the DPP from flies expressing four of the probes (Tb^{R322H}, PH-GFP, OSH2 and P4M). At time zero (first frames) in dark-adapted flies, the initial rhabdomeric localization is clearly visible, but within seconds the fluorescence from the rhabdomere pattern faded, often becoming darker than background fluorescence, reflecting translocation of the probe out of the rhabdomere due to depletion of PtdIns(4,5)P_2 and PtdIns4P by light-activated PLC. The time courses of fluorescence decay were very similar to those measured in dissociated cells expressing the respective probes (c.f. Fig. 1C). Although it is straightforward to make measurements from ROIs of such movies, it is more convenient to directly measure intensity via a photomultiplier tube (PMT), using a rectangular diaphragm to crop the area of measurement to the rhabdomere pattern (e.g. Fig. 2). Time courses derived from such measurements are similar to those made using ROI analysis of movies (e.g. Satoh et al., 2010), and allow measurements to be made in real time with high temporal resolution.

Whilst confirming the decay of fluorescence, with distinct time courses for the different probes, the PMT records also revealed additional rapid kinetic features. Firstly, there is a very rapid transient with a decay time constant of ~10-20 ms. This transient reflects R to M photoisomerization and was absent in a second flash if the visual pigment was not first photoreisomerised to the R state by long wavelength light (Fig. 2D). The rapid reduction in fluorescence is presumably because M (λ_{max} 570 nm) absorbs the emitted fluorescence more strongly than R (λ_{max} 480 nm). Interestingly, PH-GFP in particular then showed a distinct increase in fluorescence lasting ~200 ms after light onset, before the decay reflecting PtdIns(4,5)P_2 hydrolysis (Fig. 2E). Such a phase was generally absent using the other probes, and possibly reflects the initial rapid release of InsP_3 in the microvilli before it diffuses away into the cell body.

In order to confirm that the decay of the fluorescence was dependent upon hydrolysis of PtdIns(4,5)P_2 by PLC, we crossed flies expressing PH-GFP and Tb^{R332H} into a PLC null mutant background ($norpA^{P24}$). As expected, apart from the rapid transient reflecting R>M photoisomerization, there was now essentially no loss of fluorescence over time (Fig. 2C). In principle GFP fluorescence might be sensitive to other light-

induced changes in the microvillar environment, such as pH, which can be expected to become more acidic during illumination because of the protons released by the PLC reaction (Huang et al., 2010). However, similar measurements from flies expressing other GFP-tagged proteins in the microvilli (including TRPL, INAD and Kir2.1) showed little or no dynamic signal (<5%) apart from the R/M transient.

Intensity dependence of phosphoinositide depletion.

These results indicate that PtdIns(4,5)P_2 and PtdIns4P are substantially depleted in wild-type flies by saturating blue illumination. In order to measure phosphoinositide turnover in response to more physiological light regimes, we used a three pulse paradigm (Fig. 3). Flies were first exposed to a photoequilibrating 2-4 s flash of green illumination (545 ± 50 nm) that leaves most (>95%) of the visual pigment in the R state, and then dark-adapted for 2 minutes. The flies were then pre-adapted for 30 s with different intensities of the same green light and the instantaneous fluorescence in the DPP measured with blue excitation after a negligible delay (200 ms). M was then again reconverted to R by photoequilibrating green light and the cycle repeated, each time varying the intensity of the pre-adaptation, which was calibrated in terms of effectively absorbed photons by measuring the rate at which it photoreisomerised M to R (see methods and Fig. S4). Data were normalised between F_{max} (fluorescence intensity after 2 minutes dark-adaptation) and F_{min} (intensity after prolonged exposure to saturating blue excitation. The relative amount of PtdInsP_n species remaining the in the rhabdomere after maximum depletion (i.e. corresponding to F_{min}) is not known with certainty: however, there is unlikely to be much residual PtdIns(4,5)P_2 because the DPP images (e.g. Fig 2A) show that fluorescence of Tb ^{R332H} dropped to levels below background and similar to levels in the central R7 rhabdomere which, because of the cell-specific promoter used (Rh1) used, did not express any probe. This would also accord with previous measurements using the PtdIns(4,5)P_2 sensitive Kir2.1 channel in which channel activity was suppressed to < 5-10% of control levels by PtdIns(4,5)P_2 depleting stimuli (Hardie et al., 2004). By contrast DPP images of P4M generally revealed significant residual fluorescence above background and R7 suggesting that PtdIns4P may not have been quite so severely depleted (Fig. 2B).

All probes behaved in broadly similar fashion, translocating from the rhabdomere progressively with increasing pre-adaptation intensity (Fig. 3B). Tb^{R332H} and PH-GFP showed 50% depletion at intensities equivalent to ~10 effectively absorbed photons/microvillus/sec (or ~ 300,000 photons per sec per photoreceptor), approximating bright daylight conditions (Juusola and Hardie, 2001). PH-GFP began to leave the rhabdomeres at slightly lower intensities than Tb^{R332H}. Again this may reflect PH-GFP's high affinity for Ins*P*$_3$. Thus, even before significant depletion of PtdIns(4,5)*P*$_2$, finite amounts of $InsP_3$ are generated in the rhabdomeres, and will presumably diffuse into the cell body acting as a high affinity sink for PH-GFP.

OSH2, which binds PtdIns4*P* and PtdIns(4,5)*P*$_2$ with similar affinity, was somewhat more resistant to depletion, but the PtdIns4*P*-specific P4M probe was most resistant with only partial depletion observed at the highest green intensities tested, which were at least an order of magnitude brighter than brightest environmental light levels. Together these results indicate that a substantial ($\geq$ 50%) reserve of PtdIns(4,5)*P*$_2$ and most of the PtdIns4*P* remain in the microvilli of wild-type flies even under the brightest natural conditions.

Phosphoinositide depletion in *trp* and PKC mutants.

The transient receptor potential (*trp*) mutant is so-called because its response to maintained illumination decays to baseline over a few seconds (e.g. Fig. 7B). From experiments using Kir2.1 channels as biosensors, we previously proposed that the *trp* decay phenotype reflected depletion of PtdIns(4,5)*P*$_2$ due to failure of Ca^{2+} dependent inhibition of PLC by Ca^{2+} influx via the TRP channels (Hardie et al., 2001). To test this *in vivo* with independent methodology, we expressed the probes in *trp* mutants and again quantified their time- and intensity-dependent translocation.

Consistent with enhanced PtdIns(4,5)*P*$_2$ hydrolysis in *trp* mutants, Tb^{R332H} , OSH2 and P4M all translocated significantly more rapidly ($P < 0.005$, 2-tailed unpaired *t*-test) in *trp* mutant backgrounds (Fig. 2G). Interestingly however, PH-GFP translocation was actually slightly slower. This may again reflect its affinity for $InsP_3$, which should continue to be produced within the microvilli for longer if PLC is not rapidly inactivated. Most strikingly, when we determined the intensity dependence of depletion, all probes translocated out of the rhabdomeres at ~100 times lower

intensities in *trp* than in wildtype flies (Fig. 3B), confirming the profound PtdIns(4,5)P_2 depletion previously proposed to underlie the *trp* decay phenotype (Hardie et al., 2004; Hardie et al., 2001), and extending this finding now to PtdIns4*P*. Nevertheless, the overall extent of translocation (F_{max}/F_{min} ratio) following prolonged ($\geq$ 30s) blue excitation was similar in wild-type and *trp* backgrounds for both the PtdIns(4,5)P_2 and the PtdIns4*P* binding probes (Fig. 2H). This indicates that in the PDA state (after photoequilibrating blue illumination) PtdIns4*P* and PtdIns(4,5)P_2 are depleted in wild-type flies to a similar extent to that observed in *trp* mutants.

The depletion of PtdIns(4,5)P_2 in *trp* mutants has been attributed to the failure of Ca^{2+} dependent inhibition of PLC, but how Ca^{2+} inhibits PLC is unclear. Previously we proposed that the inhibition was mediated by protein kinase C (PKC) encoded by the *inaC* gene (Gu et al., 2005). If this is the case we predicted that in *inaC* mutants, PtdIns(4,5)P_2 should also be depleted at much lower intensities than in wild-type flies. Indeed, PtdIns(4,5)P_2 depletion monitored using Tb^{R332H} in the PKC null mutant $inaC^{P209}$ was at least as severe as in the *trp* mutant, even showing some loss of probe from the rhabdomere pattern in the DPP at intensities below the threshold for depletion in a *trp* background (Fig. 3C).

In *trp* mutants the remaining TRPL channels still permeate significant amounts of Ca^{2+} before the response decays to baseline. To investigate PtdIns(4,5)P_2 depletion in the absence of any Ca^{2+} influx, we expressed Tb^{R332H} on a *trpl*;*trp* double mutant background lacking all light-sensitive channels. PtdIns(4,5)P_2 was now depleted even more sensitively (~10-fold) than in single *trp* mutants, or in *inaC* mutants (Fig. 3C). The rate of Tb^{R332H} translocation on a *trpl*;*trp* background was also very significantly accelerated with respect to the single *trp* mutant, with a time constant of <1 s (0.87 ± 0.46 s n = 7; Fig 2G).This suggests that in addition to inhibition mediated by PKC, there is also a PKC-independent, Ca^{2+} dependent inhibition of PLC.

Phosphoinositide resynthesis

Previous measurements using Kir2.1 channels as electrophysiological biosensors indicated that, following depletion, PtdIns(4,5)P_2 is resynthesised over a time course of a couple of minutes in whole-cell voltage clamped photoreceptors (Hardie et al., 2004). We tracked phosphoinositide resynthesis *in vivo* in intact flies by measuring

the time course with which fluorescence returned to the rhabdomeres following depletion. Flies were first exposed to 30-60 s blue illumination, resulting in maximum loss of probe from the DPP; M was then photoreisomerized to R with a 2-4 s photoequilibrating flash of long wavelength light and after a variable period of dark adaptation, fluorescence in the DPP was measured with another blue stimulus (Fig. 4). The cycle was repeated, each time varying the time in the dark, until the most of the fluorescence in the rhabdomeres had recovered.

a) PtdIns(4,5)P_2 probes

The PtdIns(4,5)P_2/InsP_3 binding PH-GFP returned very quickly with a half-time (t½) of only 15 s. Tb^{R332H} returned with a t ½ of ~40 s, which is close to that reported using $Kir2.1^{R228Q}$ (~50s) in whole-cell recordings (Hardie et al., 2004). Tb^{R332H} returned with a similar time course on both wild-type and *trp* mutant backgrounds (Fig. 4D); however, PH-GFP returned significantly more slowly on a *trp* mutant background (t ½ ~25 s c.f. 15 s in wild-type), possibly reflecting slow cytosolic clearance of the excess InsP_3 generated in *trp* (because of prolonged PLC activity). On a longer time scale, Tb^{R332H} returned with two distinct time constants, reaching ~75% recovery in 1-2 minutes, but requiring ~1 hour for complete recovery (Fig. 4C). We looked for a functional correlate of this in the recovery of light sensitivity in ERG recordings from *trp* mutants after inducing response decay with prolonged (20 s) saturating illumination. Indeed, we found that whilst most sensitivity to light recovered relatively rapidly (~80% within ~2 minutes), there was a second slower phase of recovery with sensitivity continuing to increase for up to one hour after the initial PtdIns(4,5)P_2 depletion (Fig. 4C). A two exponential fit to the data yielded very similar time constants (35 s and 776 s) to those seen using Tb^{R332H} (38 s and 642 s).

Whether measured in wild-type or *trp*, the time course for PtdIns(4,5)P_2 resynthesis in the dark seemed quite slow compared to the rate of depletion, and we wondered whether resynthesis might be accelerated during illumination by Ca^{2+} or other products of the transduction cascade. To test this we measured recovery time courses using Tb^{R332H} (in a wild-type background), both in the dark and in the presence of background intensities sufficient to generate a sizeable electrical light response (with associated Ca^{2+} influx). Over a ~100-fold range of intensities (~0.1 – 10 photons/microvillus/second), from those too low to induce any PtdIns(4,5)P_2

depletion to those inducing >50% PtdIns(4,5)P_2 depletion, we found no indication for an acceleration of resynthesis, suggesting the rate-limiting step(s) for PtdIns(4,5)P_2 resynthesis are not modulated by Ca^{2+} or other products of the phototransduction cascade (Fig. S3).

b) PtdIns4P probes

Of the three PtdIns4*P* probes tested, OSH1 and P4M both recovered quickly, with t ½ of 26s (OSH1) and 12 s (P4M) respectively. By contrast OSH2 returned much more slowly (t½ 55 s). OSH2 has the highest affinity of these probes (Yu et al., 2004), and also exhibited the slowest rate of translocation from rhabdomere to cytosol (Fig. 2), suggesting that its translocation might be compromised by high affinity, or non-specific binding. OSH1 had relatively rapid recovery kinetics; however, because, like OSH2, it is compromised by also binding to PtdIns(4,5)P_2 and also gave a weak $F_{rh}/_{cyt}$ ratio (Fig. 1), we consider the PtdIns4*P*-specific P4M probe to be the most reliable reporter.

P4M behaved in a broadly similar manner when expressed in *trp* mutants; however, recovery was ~ 2-fold slower (t½ 23 s). The slower recovery might reflect more profound PtdIns depletion during blue illumination in *trp* mutants necessitating replenishment from ER, whilst PtdIns4*P* in wild-type might be at least partially restored from a PtdIns reserve remaining in the rhabdomere.

PtdIns(4,5)*P*$_2$ recycling mutants

The first enzyme in the canonical PtdIns(4,5)P_2 recycling pathway is DAG kinase (DGK), which converts DAG to phosphatidic acid (PA, Fig. 5D). In *Drosophila* photoreceptors, DGK is encoded by the *rdgA* gene (Masai et al., 1993); however, there is little direct evidence that it is required for PtdIns(4,5)P_2 resynthesis in the photoreceptors, and in principle there are alternative sources of PA, such as from phosphatidyl choline (PC) via phospholipase D (e.g. Raghu et al., 2009). Because severe *rdgA* mutants have profound early onset retinal degeneration due to constitutive Ca^{2+} influx via TRP channels, we investigated PtdIns(4,5)P_2 resynthesis in *rdgA*;;*trp* double mutants, in which degeneration is largely rescued (Raghu et al., 2000). When expressed in dark-adapted $rdgA^{1}$;;trp^{343} double mutants we detected fluorescence of Tb^{R332H} in the rhabdomeres, which decayed as usual during blue

illumination. However, subsequent return of Tb^{R332H} in the dark (following photoreisomerization of M to R) was greatly slowed (t ½ ~13 ± 5.5 min n = 7; Fig. 5). Since *rdgA*^{1} is not a null allele, we cannot conclude whether the eventual recovery of PtdIns(4,5)P_2 was due to residual DGK function or whether alternative, slower pathways were responsible. Both absolute fluorescence intensities and F_{max}/F_{min} ratios in *rdgA;;trp* were also reduced. On the assumption that PtdIns(4,5)P_2 was ultimately depleted to at least the same extent by blue excitation in *rdgA;;trp*, comparison of F_{max}/F_{min} values with controls should provide information on the initial dark-adapted level of PtdIns(4,5)P_2. This comparison suggested that resting PtdIns(4,5)P_2 was at least ~2-fold reduced compared to controls (Fig. 5B).

Another gene presumed to be required for PtdIns(4,5)P_2 recycling is *rdgB*, which encodes a phosphatidyl inositol transfer protein (PITP) believed to be required for transporting PI from the ER to the plasma membrane (Milligan et al., 1997; Vihtelic et al., 1993). Recently RDGB and a mammalian homologue (Nir2) have also been proposed to transport PA in the opposite direction (Kim et al., 2015; Yadav et al., 2015). Mutants of *rdgB* undergo severe light-dependent retinal degeneration, but have wild-type morphology when reared in the dark. *rdgB* mutations have also been shown to result in prolonged response inactivation (Milligan et al., 1997) and to impair resynthesis of PtdIns(4,5)P_2 in dissociated cells using Kir2.1 channels as a biosensor (Hardie et al., 2001). When Tb^{R332H} was expressed in a protein null *rdgB* mutant (*rdgB*^{2}), the rhabdomere pattern in the DPP of dark-reared flies again showed clear fluorescence, which decayed during blue excitation. However, recovery of fluorescence was profoundly slowed, recovering over a period of ~1 hour with a time course (t ½ 18.6 ± 5.9 min n = 8) even slower than that observed in *rdgA* (Fig. 5C). Based on the F_{max}/F_{min} ratios, the fully dark-adapted level of PtdIns(4,5)P_2 in *rdgB*^{2} was ~2.2 fold reduced compared to controls (Fig. 5B). Experiments using the hypomorphic allele *rdgB*^{9} indicated a similar, but slightly less severe slowing of PtdIns(4,5)P_2 resynthesis (t ½ 13.1 ± 2.0 min, n = 9) and reduction in F_{max}/F_{min} values (2.1 fold).

We also confirmed that both DGK and PITP were required for replenishing PtdIns4*P* in the rhabdomere by expressing P4M on *rdgA*^{1} and *rdgB*^{2} backgrounds. Following depletion, fluorescence in both *rdgA*^{1}*;;trp*,P4M and *rdgB*^{2};P4M flies again recovered only slowly over a period of ~ 1 hour (t½ ~9 min in *rdgA*^{1}*;;trp* and ~12 min in *rdgB*^{2}). Based on the F_{max}/F_{min} ratios, the fully dark-adapted level of PtdIns4*P* in both *rdgA*^{1}*;;trp* and *rdgB*^{2} was also substantially (~2.5-fold) reduced (Fig 5B).

Simultaneous fluorescence and ERG recordings

Both the intensity dependence of PtdIns(4,5)P_2 depletion and the time course of its recovery appear similar to measurements previously made of sensitivity to light in *trp* mutants using electrophysiological recordings (Cosens and Manning, 1969; Hardie et al., 2004; Hardie et al., 2001; Minke, 1982). However, these were made using different experimental conditions and illumination regimes. In order to test this relationship more rigorously we made simultaneous recordings of electroretinograms (ERG) and Tb^{R332H} fluorescence, so that PtdIns(4,5)P_2 levels could be directly compared with sensitivity to light in the same fly. Strikingly, sensitivity to light in *trp* mutants was suppressed by pre-illumination with essentially identical intensity dependence to that of PtdIns(4,5)P_2 depletion monitored by Tb^{R332H}, and recovered with an almost identical time course (Figs 6B and 7B). These results represent compelling quantitative confirmation that the *trp* phenotype reflects PtdIns(4,5)P_2 depletion and indicate that the response to light in *trp* (mediated by TRPL channels) can also be used as a sensitive indicator of PtdIns(4,5)P_2 levels.

We also made simultaneous recordings of ERG and fluorescence in wild-type flies, where the response is predominantly mediated by TRP channels (Figs 6A and 7A). Although Tb^{R332H} returned to the rhabdomere with a similar time course to that observed in *trp* mutants, sensitivity to light recovered significantly more quickly. Furthermore, suppression of sensitivity to light by pre-adapting illumination was much less than the extent of PtdIns(4,5)P_2 depletion (e.g. ~70% ERG amplitude remaining after PtdIns(4,5)P_2 had been depleted to 10% of original level). This distinction indicates that TRP channels can still be robustly activated when PtdIns(4,5)P_2 levels are much lower than is the case for TRPL channels, and is likely to be a contributory factor to the "transient receptor potential" response decay

phenotype whereby the response decays to baseline as PtdIns(4,5)P_2 is depleted due to failure of Ca^{2+} dependent inhibition of PLC

Time course of synthesis of PtdIns(4,5)*P*$_2$ from PtdIns4*P*.

Somewhat surprisingly, recovery of Tb^{R332H} (t½ ~40 s) was much slower than for P4M (~12 s), suggesting that conversion of PtIns4*P* to PtdIns(4,5)P_2 by PtdIns4*P* 5-kinase is the slowest, and rate-limiting step in the photoreceptors' phosphoinositide cycle (Fig. 4). In order to obtain an independent estimate of this rate, we expressed the *Ciona intestinalis* voltage-sensitive lipid phosphatase (CiVSP) in the photoreceptors. This unique voltage dependent enzyme rapidly dephosphorylates PtdIns(4,5)P_2 to PtdIns4*P* at positive membrane voltages, providing an opportunity to measure how fast PtdIns(4,5)P_2 is resynthesised from PtdIns4*P* (Falkenburger et al., 2010; Iwasaki et al., 2008; Murata et al., 2005). To exploit this tool, experiments must be performed under voltage clamp conditions, and rather than using PH probes to monitor PtdIns(4,5)P_2 levels, we now simply used the response to light mediated by TRPL channels, which, as shown above (Figs 6 and 7), can also provide a valid measure of PtdIns(4,5)P_2.

Photoreceptors from dissociated ommatidia expressing Ci-VSP were whole-cell voltage clamped, replacing K^+ with Cs^+ and TEA^+ in the pipette solution to block voltage dependent potassium channels, and exposed to La^{3+} to block TRP channels, leaving a light-induced current mediated exclusively by TRPL channels (phenocopying the *trp* mutation). After recording control responses to dim test flashes at resting potential (-70 mV), voltage steps were applied between -10 and +110 mV and the response to the same test flash recorded on return to -70 mV (Fig. 8A,B). The response to the second flash was systematically suppressed as a function of voltage, closely matching the known voltage dependence of Ci-VSP (Falkenburger et al., 2010; Murata and Okamura, 2007). Controls in wild-type photoreceptors showed no such suppression by depolarizing steps. The suppression of sensitivity to light can be attributed to VSP activity depleting PtdIns(4,5)P_2, and the rate of PtdIns(4,5)P_2 resynthesis from PtdIns4*P* can thus be estimated from the time course with which sensitivity to light recovered. Responses following a near saturating voltage step (5-10 s to +90 mV) were suppressed to ~20% of their initial value and recovered, typically to within ~80% of control, over a period of 1-2 minutes (Fig. 8C). We then depleted PtdIns(4,5)P_2 to the same extent in the same cell, by using light adjusted in

intensity in order to induce a similar initial suppression. The recovery time course from the light-induced and VSP-induced suppression overlapped closely, supporting the idea that conversion of PtIns4*P* to PtdIns(4,5)P_2 by PtdIns4*P* 5- kinase indeed represents the rate-limiting step (Fig. 8D) .

Discussion

Since the introduction of PLCδ1-PH GFP (Stauffer et al., 1998; Varnai and Balla, 1998), fluorescently tagged lipid binding domains have been widely used to monitor phosphoinositide turnover (review Balla et al., 2009), but in most cases their use has been restricted to cultured cells. In the present study we systematically and quantitatively studied the translocation of a palette of PtdIns(4,5)P_2 and PtdIns4P specific probes *in vivo* in *Drosophila* photoreceptors in response to accurately calibrated stimulation. The deep pseudopupil (DPP) in particular provides a rare opportunity to track probes in a subcellular compartment (rhabdomere) in completely intact animals over extended time periods. Whilst independently confirming conclusions from previous studies using Kir2.1 channels as electrophysiological biosensors (Hardie et al., 2004; Hardie et al., 2001), the present study has provided substantial new insight into the dynamics of phosphoinositide turnover *in vivo*. The optical *in vivo* recordings are straightforward to perform, require only modest equipment and could well be used for relatively high throughput screening. In the following we discuss the relative merits of the different probes and the implications of the results for understanding phosphoinositide turnover *in vivo* under defined physiological conditions in this genetically tractable model system.

PtdIns(4,5)P_2 probes

The Tubby PH domain binds PtdIns(4,5)P_2, PtdIns(3,4)P_2, and PtdIns(3,4,5)P_3, but not PtdIns(3,5)P_2, PtdIns(4)P, PtdIns or Ins(1,4,5)P_3 (Brown et al., 2007; Santagata et al., 2001). Compared to PtdIns(4,5)P_2, only trace amounts of PtdIns(3,4)P_2, and PtdIns(3,4,5)P_3 are likely to be present in the plasma (microvillar) membrane, and hence Tubby should effectively function as a specific PtdIns(4,5)P_2 reporter. However, as noted in other systems (e.g. Quinn et al., 2008; Szentpetery et al., 2009), the affinity of wild-type Tubby protein appears to be too high to allow rapid dissociation from the membrane, and in photoreceptors it translocated too slowly to be useful. By contrast, the Tb^{R332H} mutant appeared to faithfully report PtdIns(4,5)P_2 levels, and its behaviour – both intensity dependence of translocation and time course of recovery - closely matched previous data obtained from whole-cell patch clamp using the $Kir2.1^{R228H}$ mutant, which was similarly mutated to reduce effective affinity to match the physiological range (Hardie et al., 2004), as well as sensitivity to light in the *trp* mutant (Figs 6 and 7).

The widely used PLCδ1 PH domain (PH-GFP) gave broadly similar results to Tb^{R332H}, but we noted several discrepancies. These included greater sensitivity to translocation at lower light levels, the very rapid time constant of translocation out of the rhabdomeres, an unusually rapid return to the rhabdomeres, a transient increase at the onset of blue excitation and paradoxically slower translocation out of the rhabdomeres in *trp* mutants despite the expectation of more rapid PtdIns(4,5)P_2 depletion. As discussed above, most of these differences seem attributable to PH-GFP's affinity for $InsP_3$ (Hirose et al., 1999; Nash et al., 2001; Szentpetery et al., 2009); how*e*ver, the more rapid recovery following PtdIns(4,5)P_2 depletion might imply that PH-GFP has a higher affinity for PtdIns(4,5)P_2 than Tb^{R332H} , although to our knowledge there are no direct data on their relative affinities. Whilst a useful probe for PLC activity, we therefore suggest that PLCδ1 PH should be used with caution as a reporter of PtdIns(4,5)P_2 levels, in this system at least.

The very rapid translocation of PLCδ1 PH-GFP with a time constant of ~1 s (Fig. 1) is probably strongly influenced by the generation of $InsP_3$ in the microvilli diffusing rapidly into the cytosol to act as a sink. An alternative suggestion would be that the slower translocation of Tb^{R332H} and other probes reflects slower inherent diffusion of these probes (e.g. because of higher affinity or non-specific binding). However, this seems unlikely because in *trpl*;*trp* mutants, where net PtdIns(4,5)P_2 hydrolysis is maximised due to the lack of all Ca^{2+} influx (Fig. 3C), Tb^{R332H} translocated just as rapidly as PH-GFP (Fig. 2G). Nevertheless, even this rapid translocation may ultimately be limited by diffusion as other estimates of PtdIns(4,5)P_2 depletion rates in the absence of all Ca^{2+} influx have suggested even more rapid hydrolysis. These include the rate of Shab (Kv2.1) channel modulation by light-induced PtdIns(4,5)P_2 depletion (Krause et al., 2008), the rate of photomechanical contraction attributed to PtdIns(4,5)P_2 depletion (Hardie and Franze, 2012) and the time course of acidification attributed to proton release by PLC (Huang et al., 2010). All these approaches suggest that PtdIns(4,5)P_2 can be largely depleted within ~200 ms by saturating light in the absence of Ca^{2+} dependent feedback.

During preparation of this MS, (Chakrabarti et al., 2015) made measurements interpreted as PtdIns(4,5)P_2 resynthesis, using PH-GFP imaged in the DPP, but

reported ~10-fold slower time courses of recovery than those found here with PH-GFP (t½ 2-3 min c.f. ~15s). A likely reason for this discrepancy is that they measured recovery of fluorescence (following blue excitation) in the presence of continuous red illumination, which was used to reconvert M to R. Because PtdIns(4,5)P_2 remains depleted following blue excitation until M is photoreisomerised (Fig. 4B), it seems possible that the slow time courses reported by these authors represented the time taken for M to R reconversion by their red illumination. By contrast we rapidly reconverted M to R with a brief (2-4 s) pulse of intense red/orange light before measuring the resynthesis time course in the dark.

PtdIns4*P* probes

Of the three PtdIns4*P* probes tested our results suggest that P4M is the most reliable. Until recently OSH1 and OSH2 were favoured probes for PtdIns4*P*; however, both also bind to PtdIns(4,5)P_2 with similar affinity (Yu et al., 2004). By contrast the P4M domain (from *Legionella* SidM) is highly specific for PtdIns4*P* (Brombacher et al., 2009). Its affinity also appears well matched to the physiological levels of PtdIns4*P* in cultured cells because it responds to both increases and decreases in the lipid's abundance (Hammond et al., 2014). Here, the close quantitative correspondence of intensity dependence of Tb^{R332H} and P4M translocation (Fig. 4) in *trp* mutants strongly suggests that the affinity of P4M is well matched to the range of physiological levels of PtdIns4*P* in the photoreceptors as well.

The intensity dependence of OSH2 and OSH1 (not shown) translocation in wild-type photoreceptors was intermediate between the P4M and Tb^{R332H} probes (Fig. 3), consistent with their translocation being determined by a combination of PtdIns4*P* and PtdIns(4,5)P_2 binding. OSH2 also displayed a very sluggish recovery time course and slow decay time constant suggesting that its translocation may be compromised by high affinity/non-specific binding. Translocation of OSH1, which has ~3-fold lower affinity than OSH2, may provide more plausible time course information, but its dual affinity for PtdIns4*P* and PtdIns(4,5)P_2 as well as its relatively small F_{max}/F_{min} signal (~1.3 in dissociated ommatidia) compromise its usefulness.

Phosphoinositide turnover under physiological conditions

The present results document intensity dependence and resynthesis time course of both PtdIns(4,5)P_2 and PtdIns4P under physiological conditions in wild-type backgrounds, and do so *in vivo* using completely intact living flies and illumination calibrated in terms of effectively absorbed photons. The results indicate that PtdIns(4,5)P_2 can be depleted by only about ~50% at intensities expected to be experienced under brightest daylight conditions. Measurements using P4M indicated that PtdIns4P levels were virtually unaffected at physiologically relevant levels and only ~50% depleted by intensities ~10x brighter than daylight. However, a significant finding was, that during the PDA caused by saturating blue illumination, both PtdIns(4,5)P_2 and PtdIns4P appear to be depleted as extensively in wild-type as is the case in *trp* mutants and remain so until M has been reconverted to R by long wavelength illumination. Whilst these conditions would rarely, if ever, occur under natural conditions, the PDA is extensively used in *Drosophila* eye research, and it is important to realise that in this state the microvilli are very likely severely depleted of both PtdIns(4,5)P_2 and PtdIns4P.

Mutations affecting the phosphoinositide cycle

The results provide compelling confirmation of the profound depletion of PtdIns(4,5)P_2 by low light levels in *trp* mutants, and now extend this finding to PtdIns4P as well (Fig. 4) . Quantitatively, ~50% of both PtdIns(4,5)P_2 and PtdIns4P (i.e. normalized probe fluorescence) were depleted in *trp* flies at intensities equivalent to ~0.1 photons per microvillus/second (~3000 photons/photoreceptor/s). The results also quantitatively confirm a similarly, and even slightly more severe phenotype in *inaC* mutants lacking PKC. This indicates, as previously proposed (Gu et al., 2005), that Ca^{2+} influx, acting via Ca^{2+} (and DAG)-dependent PKC prevents PtdIns(4,5)P_2 depletion, by inhibition of PLC. An alternative, or complementary interpretation of these results might be that Ca^{2+} (and PKC) facilitate PtdIns(4,5)P_2 resynthesis; however, over a wide range of intensities we could find no significant effects of light adaptation (with associated Ca^{2+} influx and PKC activation) on the rate of resynthesis of PtdIns(4,5)P_2 (Fig. S3). Nevertheless, it remains unclear how PKC inhibits PLC, given that PLC is not believed to be a direct substrate for PKC in the photoreceptors (Huber et al., 1996). One possibility is via the INAD scaffolding

molecule, which is a PKC target (Voolstra et al., 2015), whilst an effect at the level of the G-protein cannot be excluded.

Ca^{2+} dependent inhibition of PLC was independently supported by the sensitive, and rapid PtdIns(4,5)P_2 depletion seen in the absence of any Ca^{2+} influx in *trpl;trp* double mutants. In fact, PtdIns(4,5)P_2 was ~1000-fold more sensitive to depletion in *trpl;trp* than in wild-type, and ~10-fold more sensitive than in *inaC* (or *trp*). This indicates an additional, eye-PKC- independent inhibition of PLC by Ca^{2+} that can also be mediated by the residual Ca^{2+} influx via TRPL channels (Fig. 4C). The mechanism for this is unknown: we cannot exclude a contribution of alternative PKC isoforms, but other possibilities might include charge interactions of the negatively charged PtdIns(4,5)P_2 headgroup with Ca^{2+} (Wang et al., 2014) or the Ca^{2+} dependent facilitation of arrestin binding to active metarhodopsin (Liu et al., 2008).

The profound slowing of PtdIns(4,5)P_2 and PtdIns4*P* resynthesis in *rgdA* and *rdgB* mutants confirm the essential involvement DAG kinase and PITP in PtdIns(4,5)P_2 resynthesis. Significantly reduced F_{max} and F_{max}/F_{min} ratios also suggest that the absolute level of PtdIns(4,5)P_2 and PtdIns4*P* in the rhabdomeres of both these mutants was substantially reduced (~2-3 fold). Despite the profoundly slowed recovery in these mutants, eventually some PtdIns(4,5)P_2 was replenished in both *rdgA*[1] (a severe hypomorph) and *rdgB*[2] (reportedly a protein null), raising the possibility of alternative pathways for resynthesis. In this respect it is perhaps significant that a minor slow component of PtdIns(4,5)P_2 recovery with a similar timecourse was seen in wild-type background (Fig. 4C).

PtdIns(4,5)P_2 levels and sensitivity to light

Simultaneous measurement of Tb^{R332H} fluorescence and ERG in *trp* mutants showed remarkable quantitative equivalence with respect to both intensity dependence and recovery after decay (Figs 6 and 7) suggesting that the electrical light response in *trp*, which is mediated exclusively by TRPL channels, is essentially proportional to the level of PtdIns(4,5)P_2. By contrast, the wild-type light response, which is dominated by TRP channels (Reuss et al., 1997), was relatively resistant to PtdIns(4,5)P_2 depletion. On the one hand this might imply differential sensitivity of TRP and TRPL channels to the (still unresolved) active products of PLC hydrolysis (putatively e.g.,

protons, mechanical forces, DAG or polyunsaturated fatty acids). However, an alternative (not mutually exclusive) explanation is that TRP (but not TRPL) channels are subject to a powerful non-linear Ca^{2+} dependent positive feedback (Reuss et al., 1997), which could be expected to result in full size "all-or-none" single photon responses even under conditions of reduced PtdIns(4,5)P_2.

Rate-limiting step

An unexpected finding was that the recovery of PtdIns4*P* was so fast (t½ ~12 s in wildtype and 25 s in *trp* mutant background), whilst PtdIns(4,5)P_2 recovered with a halftime of only ~45 s. This suggests that the rate-limiting step in the PtdIns(4,5)P_2 cycle in the photoreceptors is the final step, i.e. conversion of PtdIns4*P* to PtdIns(4,5)P_2 by PI4P-5kinase (Chakrabarti et al., 2015). This is contrary to limited available data in mammalian cultured cells (Falkenburger et al., 2010; Willars et al., 1998), but was supported by measurements using a voltage sensitive phosphatase (VSP), which showed that recovery of the light response following PtdIns(4,5)P_2 depletion (to PtdIns4*P*) by VSP followed a similar time course to the recovery from light-induced PtdIns(4,5)P_2 depletion (Fig. 8). The functional significance of this slow final step is unclear, but it can be speculated that it might protect the photoreceptors from total depletion of all the PtdIns and PtdIns4P reserve in the rhabdomere under conditions of bright illumination.

In conclusion, after testing a range of fluorescently tagged lipid probes we have identified Tb^{R332H} and P4M as suitable for real time monitoring of PtdIns(4,5)P_2 and PtdIns4*P* in *Drosophila* photoreceptors. Using appropriate paradigms these can be used to track and quantify phosphoinositide breakdown and resynthesis in the rhabdomeres of completely intact living flies, with a precision we believe to be unsurpassed in other systems. This approach is straightforward to implement in the fly eye, and whilst Tb^{R332H} and P4M should prove valuable for further physiological and molecular dissection of this important signalling pathway, this methodology can be readily extended to other genetically encoded fluorescent probes.

Material and methods

Flies *Drosophila melanogaster* were reared in the dark at 25ºC on standard (cornmeal/ agar/ yeast/ glucose) diet. Although probes (see below) were expressed in a white-eyed (w^{1118}) background, the mini-white gene used as a marker in the expression vector confers eye colour, which varies from pale orange to red between independent inserts of even the same transgene. Eye colour had little if any effect on normalised data; however, deeper eye colours have lower absolute fluorescence, and greater F_{max}/F_{min} ratios due to enhanced contrast of rhabdomere fluorescence (Fig. S2). In principle F_{max}/F_{min} provides information on the extent of phosphoinositide depletion or its initial level, but such comparisons were only made between flies with the same transgene insert and eye colour. Some lines were also crossed into a *cn,bw* background, resulting in white eyes despite the mini-white transgene. Transgenes were crossed into the following mutant backgrounds: $norpA^{P24}$ (null mutant for PLC, Bloomquist et al., 1988); trp^{343} , a null mutant of the TRP channel (Scott et al., 1997); $trpl^{302}$;trp^{343} a null double mutant for both light-sensitive channels; $inaC^{P209}$, a null mutant for protein kinase C (Smith et al., 1991) ; $rdgA^{1}$, a severe hypomorph of DAG kinase (Masai et al., 1993); $rdgB^{9}$ (a.k.a $rdgB^{KS222}$), a severe hypomorph, and $rdgB^{2}$ a protein null allele of a phosphatidyl inositol transfer protein (Vihtelic et al., 1993).

Transgenic flies cDNA for the PH domain of PLCδ1 (Stauffer et al., 1998) was subcloned into a plasmid containing the *trp* promoter. cDNAs for Tb^{R332H} (Quinn et al., 2008), OSH1, OSH2, P4M and *Ciona* VSP were obtained in mammalian vectors and subcloned into the pCaSper4 vector containing the *ninaE* promoter. Constructs were sequenced and confirmed at the sequencing facility of Department of Biochemistry, University of Cambridge. Concentrated plasmid DNA preps (~ 800–1000 ng/µl) were made using QIAfilter Plasmid Midi Kit and sent to Department of Genetics, University of Cambridge or BestGene Inc, USA for generation of transgenic flies by p-element transformation. Both homozygotes (two copies of transgene) and balanced lines (one copy) were used, with at least two independent transgene inserts tested for each construct, with no obvious difference in results, apart from the brighter fluorescence and deeper eye colour when using two copies of the transgenes (see supplemental material).

Imaging of dissociated ommatidia Fluorescence from isolated ommatidia was viewed with a 40x NA 1.30 oil immersion objective on a Nikon Eclipse TE300 inverted microscope, using freshly dissociated ommatidia prepared as previously described for electrophysiological patch-clamp experiments (e.g. Hardie, 1991; Hardie et al., 2002). Images were captured, typically at 1-5 frames s^{-1}, using an Orca 4.0 Flash camera (Hamamatsu). The average intensity was measured in regions of interest in rhabdomere and cytosol using Hamamatsu HC image software (e.g. Fig.1). The bath contained (in mM): 120 NaCl, 5 KCl, 10 *N*-Tris-(hydroxymethyl)-methyl-2-amino-ethanesulphonic acid (TES), 4 $MgCl_2$, 1.5 $CaCl_2$, 25 proline and 5 alanine, pH 7.15.Chemicals were ordered from Sigma-Aldrich.

Live imaging of the deep pseudopupil and calibration Fluorescence from the deep pseudopupil (DPP) of intact flies was measured as previously described (Satoh et al., 2010). Briefly, flies were fixed via head and proboscis with low melting point wax in truncated pipette tips, mounted on a micromanipulator and observed with a 20x/0.35 NA Fluor objective on the Nikon inverted microscope. The DPP from a frontal-dorsal eye region was cropped via a rectangular diaphragm (similar in size to the image frames in Fig. 2A) and sampled at up to 500 Hz using a photomultiplier tube (Cairn Research Ltd) collecting fluorescence excited by a blue (470 nm peak) ultrabright LED (Cairn Research) and imaged/measured via 515 nm dichroic and OG515 long pass filters. Fluorescence signals were sampled and analysed using pClamp10 software (Molecular Devices) and, unless otherwise stated, normalised between F_{max} (1.0) and F_{min} (0.0). Photo-reisomerization of M to R was achieved by long wavelength light delivered by an ultrabright orange/red LED (640 nm Thorlabs) via the microscope eyepiece. Calibrated green illumination (~545 nm ± 50nm), also delivered via an eyepiece adapter, came from a white ultrabright LED filtered by a GG495 nm longpass filter (Fig. S4).

Fly rhodopsin (R) absorbs maximally at 480 nm, and the metarhodopsin state (M) at ~570 nm. The two states are thermostable, photo-interconvertible and exist in a photoequilibrium determined by their photosensitivity spectra and the spectral content of illumination (Fig. S 4, and see Minke and Kirschfeld, 1979). Photoequilibration was achieved within <100 ms for the blue excitation LED (generating ~70% M, 30%

R) and 1-2 s for the orange/red LED (generating ~2%M, 98% R). The intensity of the green light used for determining the intensity dependence of phosphoinositide depletion was calibrated by measuring the rate at which it photo-isomerised M to R. Long wavelength light reflected and scattered back out of the eye is more effectively absorbed by M than it is by R. Consequently, when delivered after photoequilibration with blue light (generating ~70%M), the intensity of back-scattered long wavelength light increases as M is photoreisomerized to R with an exponential time course that provides a direct measure of the rate of photoisomerization of M to R (Fig. S4). The number of M absorptions per second per microvillus was calculated from this, assuming there are 1000 rhodopsin molecules per microvillus (Harris et al., 1977). The relative absorption of R by the same light (~6x less) was calculated by convolving the spectral distribution of the light (measured with an Ocean Optics spectrometer) with photosensitivity spectra of R and M states of the pigment, and correcting for the difference (Fig. S4).

Electrophysiology Electroretinograms (ERG) were recorded as described previously (e.g. Satoh et al., 2010) from flies immobilised with low melting point wax in truncated pipette tips, as for optical recordings, using low resistance (~10 MΩ) glass microelectrodes filled with fly Ringer (140 mM NaCl, 5 mM KCl, 1.5 mM $CaCl_2$, 4 mM $MgCl_2$) inserted into the eye. When recording ERG alone, the indifferent electrode was a similar electrode inserted into the head capsule near the ocelli. For simultaneous fluorescence and ERG recordings, the indifferent electrode was a 50 μm chloridised silver wire contacting the head via a drop of ECG conducting gel. Signals were amplified by a Neurolog NL102 DC (Digitimer) or a DAM60 preamplifier (World Precision Instruments) and sampled and analysed using pClamp software (Molecular Devices CA). Whole-cell patch clamp recordings of dissociated ommatidia were made as previously described (Hardie et al., 2001) using 10-15MΩ patch pipettes containing (in mM) 140 K gluconate, 4 MgATP, 1 NAD, 0.4 NaGTP and 10TES with the bath solution described above.

Acknowledgements. This research was supported by grants from the BBSRC (BB/M00706/1 and BB/J009253/1; RCH, C-HL,ASR) and the Cambridge-Nehru Trust (SS) . The authors wish to thanks other members of the Hardie lab for comments on the MS. cDNAs for fluorescent probes were generously provided by Tamas Balla, Gerry Hammond and Andrew Tinker and *Ciona* voltage sensitive phosphatase cDNA by Yasushi Okamura.

Author contributions

RCH designed the project, performed fluorescence measurements, ERG and patch-clamp electrophysiology. CH-L generated constructs and transgenic lines, ASR and SS performed fluorescence measurements. RCH wrote the paper with feedback from all the other authors.

References

Balla, T. 2013. Phosphoinositides: tiny lipids with giant impact on cell regulation. *Physiol Rev*. 93:1019-1137.

Balla, T., Z. Szentpetery, and Y.J. Kim. 2009. Phosphoinositide signaling: new tools and insights. *Physiology (Bethesda)*. 24:231-244.

Balla, T., and P. Varnai. 2009. Visualization of cellular phosphoinositide pools with GFP-fused protein-domains. *Current Protocols Cell Biol*. Chapter 24: 24.4.21-27.

Bloomquist, B.T., R.D. Shortridge, S. Schneuwly, M. Pedrew, C. Montell, H. Steller, G. Rubin, and W.L. Pak. 1988. Isolation of putative phospholipase C gene of Drosophila, *norpA* and its role in phototransduction. *Cell*. 54:723-733.

Brombacher, E., S. Urwyler, C. Ragaz, S.S. Weber, K. Kami, M. Overduin, and H. Hilbi. 2009. Rab1 guanine nucleotide exchange factor SidM is a major phosphatidylinositol 4-phosphate-binding effector protein of Legionella pneumophila. *J. Biol. Chem*. 284:4846-4856.

Brown, D.A., S.A. Hughes, S.J. Marsh, and A. Tinker. 2007. Regulation of M(Kv7.2/7.3) channels in neurons by PIP(2) and products of PIP(2) hydrolysis: significance for receptor-mediated inhibition. *J. Physiol*. 582:917-925.

Chakrabarti, P., S. Kolay, S. Yadav, K. Kumari, A. Nair, D. Trivedi, and P. Raghu. 2015. A dPIP5K dependent pool of phosphatidylinositol 4,5 bisphosphate (PIP2) is required for G-protein coupled signal transduction in Drosophila photoreceptors. *PLoS Genet*. 11:e1004948.

Cosens, D.J., and A. Manning. 1969. Abnormal electroretinogram from a *Drosophila* mutant. *Nature*. 224:285-287.

Di Paolo, G., and P. De Camilli. 2006. Phosphoinositides in cell regulation and membrane dynamics. *Nature*. 443:651-657.

Dolph, P.J., R. Ranganathan, N.J. Colley, R.W. Hardy, M. Socolich, and C.S. Zuker. 1993. Arrestin function in inactivation of G protein-coupled receptor rhodopsin in vivo. *Science*. 260:1910-1916.

Falkenburger, B.H., J.B. Jensen, and B. Hille. 2010. Kinetics of PIP2 metabolism and KCNQ2/3 channel regulation studied with a voltage-sensitive phosphatase in living cells. *J. Gen. Physiol*. 135:99-114.

Franceschini, N., and K. Kirschfeld. 1971. Etude optique in vivo des elements photorecepteurs dans l'oeil compose de *Drosophila*. *Kybernetik*. 8:1-13.

Gu, Y., J. Oberwinkler, M. Postma, and R.C. Hardie. 2005. Mechanisms of light adaptation in *Drosophila* photoreceptors. *Curr. Biol*. 15:1228-1234.

Hammond, G.R., M.P. Machner, and T. Balla. 2014. A novel probe for phosphatidylinositol 4-phosphate reveals multiple pools beyond the Golgi. *J. Cell Biol*. 205:113-126.

Hardie, R.C. 1991. Whole-cell recordings of the light-induced current in *Drosophila* photoreceptors: evidence for feedback by calcium permeating the light sensitive channels. *Proc. Roy. Soc Lond. B.* 245:203-210.

Hardie, R.C. 2012. Phototransduction mechanisms in *Drosophila* microvillar photoreceptors. *WIRES Membr Transp Signal* 1:WIREs Membr Transp Signal 2012, 2011:2162–2187. doi: 2010.1002/wmts.2020.

Hardie, R.C., and K. Franze. 2012. Photomechanical responses in *Drosophila* photoreceptors. *Science*. 338:260-263.

Hardie, R.C., Y. Gu, F. Martin, S.T. Sweeney, and P. Raghu. 2004. In vivo light-induced and basal phospholipase C activity in *Drosophila* photoreceptors measured with genetically targeted phosphatidylinositol 4,5-bisphosphate-sensitive ion channels (Kir2.1). *J. Biol. Chem*. 279:47773-47782.

Hardie, R.C., and M. Juusola. 2015. Phototransduction in Drosophila. *Curr. Opin. Neurobiol*. 34C:37-45.

Hardie, R.C., F. Martin, G.W. Cochrane, M. Juusola, P. Georgiev, and P. Raghu. 2002. Molecular basis of amplification in *Drosophila* phototransduction. Roles for G protein, phospholipase C, and diacylglycerol kinase. *Neuron*. 36:689-701.

Hardie, R.C., and B. Minke. 1992. The *trp* gene is essential for a light-activated Ca^{2+} channel in *Drosophila* photoreceptors. *Neuron*. 8:643-651.

Hardie, R.C., P. Raghu, S. Moore, M. Juusola, R.A. Baines, and S.T. Sweeney. 2001. Calcium influx via TRP channels is required to maintain PIP_2 levels in *Drosophila* photoreceptors. *Neuron*. 30:149-159.

Harris, W.A., D.F. Ready, E.D. Lipson, A.J. Hudspeth, and W.S. Stark. 1977. Vitamin A deprivation and Drosophila photopigments. *Nature*. 266:648-650.

Hilgemann, D.W., and R. Ball. 1996. Regulation of cardiac Na^+,Ca^{2+} exchange and KATP potassium channels by PIP_2. *Science*. 273:956-959.

Hilgemann, D.W., S. Feng, and C. Nasuhoglu. 2001. The complex and intriguing lives of PIP2 with ion channels and transporters. *Sci STKE*. 2001:RE19.

Hirose, K., S. Kadowaki, M. Tanabe, H. Takeshima, and M. Iino. 1999. Spatiotemporal dynamics of inositol 1,4,5-trisphosphate that underlies complex Ca2+ mobilization patterns. *Science*. 284:1527-1530.

Huang, J., C.H. Liu, S.A. Hughes, M. Postma, C.J. Schwiening, and R.C. Hardie. 2010. Activation of TRP channels by protons and phosphoinositide depletion in *Drosophila* photoreceptors. *Curr Biol*. 20:189-197.

Huber, A., P. Sander, A. Gobert, M. Bahner, R. Hermann, and R. Paulsen. 1996. The transient receptor potential protein (Trp), a putative store-operated Ca^{2+} channel essential for phosphoinositide-mediated photoreception, forms a signaling complex with NorpA, InaC and InaD. *Embo J*. 15:7036-7045.

Hughes, S., S.J. Marsh, A. Tinker, and D.A. Brown. 2007. PIP(2)-dependent inhibition of M-type (Kv7.2/7.3) potassium channels: direct on-line assessment of PIP(2) depletion by Gq-coupled receptors in single living neurons. *Pflugers Arch*. 455:115-124.

Iwasaki, H., Y. Murata, Y. Kim, M.I. Hossain, C.A. Worby, J.E. Dixon, T. McCormack, T. Sasaki, and Y. Okamura. 2008. A voltage-sensing phosphatase, Ci-VSP, which shares sequence identity with PTEN, dephosphorylates phosphatidylinositol 4,5-bisphosphate. *Proc. Natl. Acad. Sci. U. S. A.* 105:7970-7975.

Juusola, M., and R.C. Hardie. 2001. Light adaptation in *Drosophila* photoreceptors: I. Response dynamics and signaling efficiency at 25 degrees C. *J. Gen. Physiol*. 117:3-25.

Katz, B., and B. Minke. 2009. *Drosophila* photoreceptors and signaling mechanisms. *Frontiers Cell. Neurosci.*. 3:2.

Kim, Y.J., M.L. Guzman-Hernandez, E. Wisniewski, and T. Balla. 2015. Phosphatidylinositol-Phosphatidic Acid Exchange by Nir2 at ER-PM Contact Sites Maintains Phosphoinositide Signaling Competence. *Dev Cell*. 33:549-561.

Krause, Y., S. Krause, J. Huang, C.H. Liu, R.C. Hardie, and M. Weckstrom. 2008. Light-Dependent Modulation of Shab Channels via Phosphoinositide Depletion in Drosophila Photoreceptors. *Neuron*. 59:596-607.

Liu, C.H., A.K. Satoh, M. Postma, J. Huang, D.F. Ready, and R.C. Hardie. 2008. Ca^{2+}-dependent metarhodopsin inactivation mediated by Calmodulin and NINAC myosin III. *Neuron*. 59:778-789.

Masai, I., A. Okazaki, T. Hosoya, and Y. Hotta. 1993. Drosophila retinal degeneration A gene encodes an eye-specific diacylglycerol kinase with cysteine-rich zinc-finger motifs and ankyrin repeats. *Proc. Natl. Acad. Sci. U. S. A.* 90:11157-11161.

Meyer, N.E., T. Joel-Almagor, S. Frechter, B. Minke, and A. Huber. 2006. Subcellular translocation of the eGFP-tagged TRPL channel in Drosophila photoreceptors requires activation of the phototransduction cascade. *J. Cell Sci*. 119:2592-2603.

Milligan, S.C., J.G. Alb, R.B. Elagina, V.A. Bankaitis, and D.R. Hyde. 1997. The phosphatidylinositol transfer protein domain of Drosophila retinal degeneration B protein is essential for photoreceptor cell survival and recovery from light stimulation. *J. Cell Biol.* 139:351-363.

Minke, B. 1979. Transduction in photoreceptors with bistable pigments: intermediate processes. *Biophys. Struct. Mech*. 5:163-174.

Minke, B. 1982. Light-induced reduction in excitation efficiency in the trp mutant of Drosophila. *J. Gen. Physiol*. 79:361-385.

Minke, B., and K. Kirschfeld. 1979. The contribution of a sensitizing pigment to the photosensitivity spectra of fly rhodopsin and metarhodopsin. *J. Gen. Physiol*. 73:517-540.

Montell, C. 2012. *Drosophila* visual transduction. *Trends Neurosci*. 35:356-363.

Montell, C., and G.M. Rubin. 1989. Molecular characterization of Drosophila *trp* locus, a putative integral membrane protein required for phototransduction. *Neuron*. 2:1313-1323.

Murata, Y., H. Iwasaki, M. Sasaki, K. Inaba, and Y. Okamura. 2005. Phosphoinositide phosphatase activity coupled to an intrinsic voltage sensor. *Nature*. 435:1239-1243.

Murata, Y., and Y. Okamura. 2007. Depolarization activates the phosphoinositide phosphatase Ci-VSP, as detected in Xenopus oocytes coexpressing sensors of PIP2. *J.Physiol.* 583:875-889.

Nash, M.S., K.W. Young, G.B. Willars, R.A. Challiss, and S.R. Nahorski. 2001. Single-cell imaging of graded Ins(1,4,5)P3 production following G-protein-coupled-receptor activation. *Biochem. J*. 356:137-142.

Payrastre, B., K. Missy, S. Giuriato, S. Bodin, M. Plantavid, and M. Gratacap. 2001. Phosphoinositides : key players in cell signalling, in time and space. *Cell Signal*. 13:377-387.

Phillips, A.M., A. Bull, and L.E. Kelly. 1992. Identification of a Drosophila gene encoding a calmodulin-binding protein with homology to the trp phototransduction gene. *Neuron*. 8:631-642.

Quinn, K.V., P. Behe, and A. Tinker. 2008. Monitoring changes in membrane phosphatidylinositol 4,5-bisphosphate in living cells using a domain from the transcription factor tubby. *J. Physiol.*. 586:2855-2871.

Raghu, P., E. Coessens, M. Manifava, P. Georgiev, T. Pettitt, E. Wood, I. Garcia-Murillas, H. Okkenhaug, D. Trivedi, Q. Zhang, A. Razzaq, O. Zaid, M. Wakelam, C.J. O'Kane, and N. Ktistakis. 2009. Rhabdomere biogenesis in Drosophila photoreceptors is acutely sensitive to phosphatidic acid levels. *J Cell Biol*. 185:129-145.

Raghu, P., K. Usher, S. Jonas, S. Chyb, A. Polyanovsky, and R.C. Hardie. 2000. Constitutive activity of the light-sensitive channels TRP and TRPL in the *Drosophila* diacylglycerol kinase mutant, *rdgA*. *Neuron*. 26:169-179.

Reuss, H., M.H. Mojet, S. Chyb, and R.C. Hardie. 1997. In vivo analysis of the *Drosophila* light-sensitive channels, TRP and TRPL. *Neuron*. 19:1249-1259.

Rohacs, T. 2009. Phosphoinositide regulation of non-canonical transient receptor potential channels. *Cell Calcium*. 45:554-565.

Santagata, S., T.J. Boggon, C.L. Baird, C.A. Gomez, J. Zhao, W.S. Shan, D.G. Myszka, and L. Shapiro. 2001. G-protein signaling through tubby proteins. *Science*. 292:2041-2050.

Satoh, A.K., H. Xia, L. Yan, C.H. Liu, R.C. Hardie, and D.F. Ready. 2010. Arrestin translocation is stoichiometric to rhodopsin isomerization and accelerated by phototransduction in *Drosophila* photoreceptors. *Neuron*. 67:997-1008.

Scott, K., Y.M. Sun, K. Beckingham, and C.S. Zuker. 1997. Calmodulin regulation of *Drosophila* light-activated channels and receptor function mediates termination of the light response in vivo. *Cell*. 91:375-383.

Smith, D.P., R. Ranganathan, R.W. Hardy, J. Marx, T. Tsuchida, and C.S. Zuker. 1991. Photoreceptor deactivation and retinal degeneration mediated by a photoreceptor-specific protein-kinase-C. *Science*. 254:1478-1484.

Stauffer, T.P., S. Ahn, and T. Meyer. 1998. Receptor-induced transient reduction in plasma membrane PtdIns(4,5)P-2 concentration monitored in living cells. *Curr. Biol*. 8:343-346.

Szentpetery, Z., A. Balla, Y.J. Kim, M.A. Lemmon, and T. Balla. 2009. Live cell imaging with protein domains capable of recognizing phosphatidylinositol 4,5-bisphosphate; a comparative study. *BMC Cell Biol*. 10:67.

Varnai, P., and T. Balla. 1998. Visualization of phosphoinositides that bind pleckstrin homology domains: calcium- and agonist-induced dynamic changes and relationship to myo-[3H]inositol-labeled phosphoinositide pools. *J. Cell Biol*. 143:501-510.

Vihtelic, T.S., M. Goebl, S. Milligan, J.E. O'Tousa, and D.R. Hyde. 1993. Localization of Drosophila retinal degeneration B, a membrane-associated phosphatidylinositol transfer protein. *J. Cell Biol*. 122:1013-1022.

Voolstra, O., P. Spat, C. Oberegelsbacher, B. Claussen, J. Pfannstiel, and A. Huber. 2015. Light-dependent phosphorylation of the Drosophila inactivation no afterpotential D (INAD) scaffolding protein at Thr170 and Ser174 by eye-specific protein kinase C. *PLoS One*. 10:e0122039.

Wang, Y.H., D.R. Slochower, and P.A. Janmey. 2014. Counterion-mediated cluster formation by polyphosphoinositides. *Chem. Phys. Lipids*.182:38-51

Willars, G.B., S.R. Nahorski, and R.A. Challiss. 1998. Differential regulation of muscarinic acetylcholine receptor-sensitive polyphosphoinositide pools and consequences for signaling in human neuroblastoma cells. *J. Biol. Chem*. 273:5037-5046.

Yadav, S., K. Garner, P. Georgiev, M. Li, E. Gomez-Espinosa, A. Panda, S. Mathre, H. Okkenhaug, S. Cockcroft, and P. Raghu. 2015. RDGBalpha, a PI-PA transfer protein regulates G-protein coupled PtdIns(4,5)P2 signalling during Drosophila phototransduction. *J. Cell. Sci*. doi 10.1242/jcs.173476

Yau, K.W., and R.C. Hardie. 2009. Phototransduction motifs and variations. *Cell*. 139:246-264.

Yin, H.L., and P.A. Janmey. 2003. Phosphoinositide regulation of the actin cytoskeleton. *Annu. Rev. Physiol*. 65:761-789.

Yu, J.W., J.M. Mendrola, A. Audhya, S. Singh, D. Keleti, D.B. DeWald, D. Murray, S.D. Emr, and M.A. Lemmon. 2004. Genome-wide analysis of membrane targeting by S. cerevisiae pleckstrin homology domains. *Mol. Cell*. 13:677-688.

FIGURES

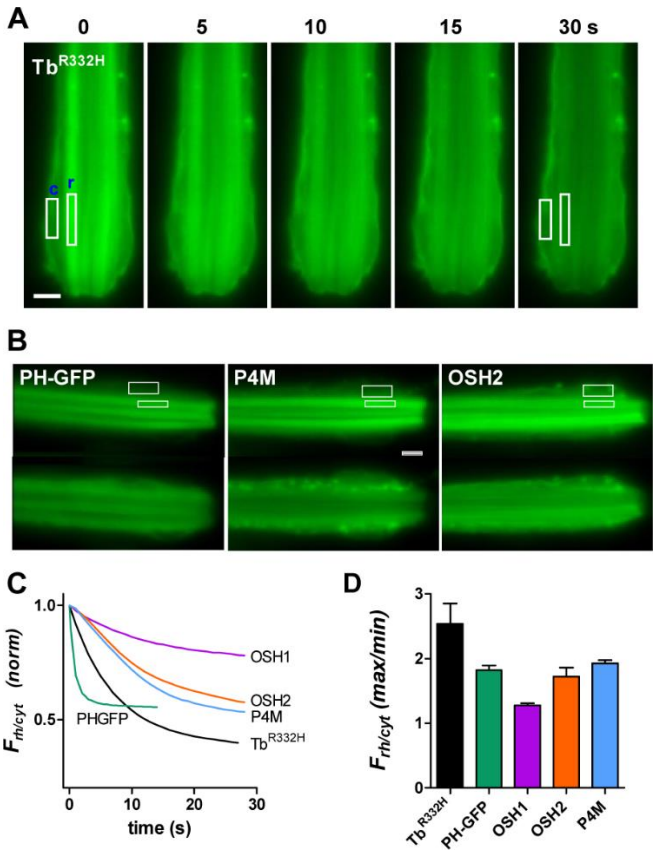

Figure 1 Translocation of fluorescent probes in dissociated ommatidia

(A) Fluorescent images from initially dark-adapted dissociated ommatidium expressing Tb^{R332H} immediately at onset of blue excitation (t = 0) and 5, 10, 15 and 30 s later. Fluorescence was initially strongest in the rhabdomeres (r), but rapidly translocated to cell body and plasma membrane (c): white boxes show typical ROIs used for measurement. (**B**) Fluorescence from dissociated ommatidia of flies expressing, PLCδ1-PHGFP (PH-GFP), P4M and OSH2. Top image in each pair at time = 0; bottom image, 30 s later. Following translocation PH-GFP localised to cytosol; P4M and OSH2 also localised to endomembranes. Scale bars 5 μm. (**C**) Time course of translocation measured as normalised ratio of fluorescence from regions of interest (e.g. boxes in A and B) in rhabdomere and cytosol ($F_{rh/cyt}$). Each trace is the mean of measurements from 5-12 ommatidia. (**D**) Extent of fluorescence decay ($F_{rh/cyt}$ max/min) expressed as ratio between $F_{rh/cyt}$ at time zero and after 30 s illumination (mean ± s.e.m. n = 5-12).

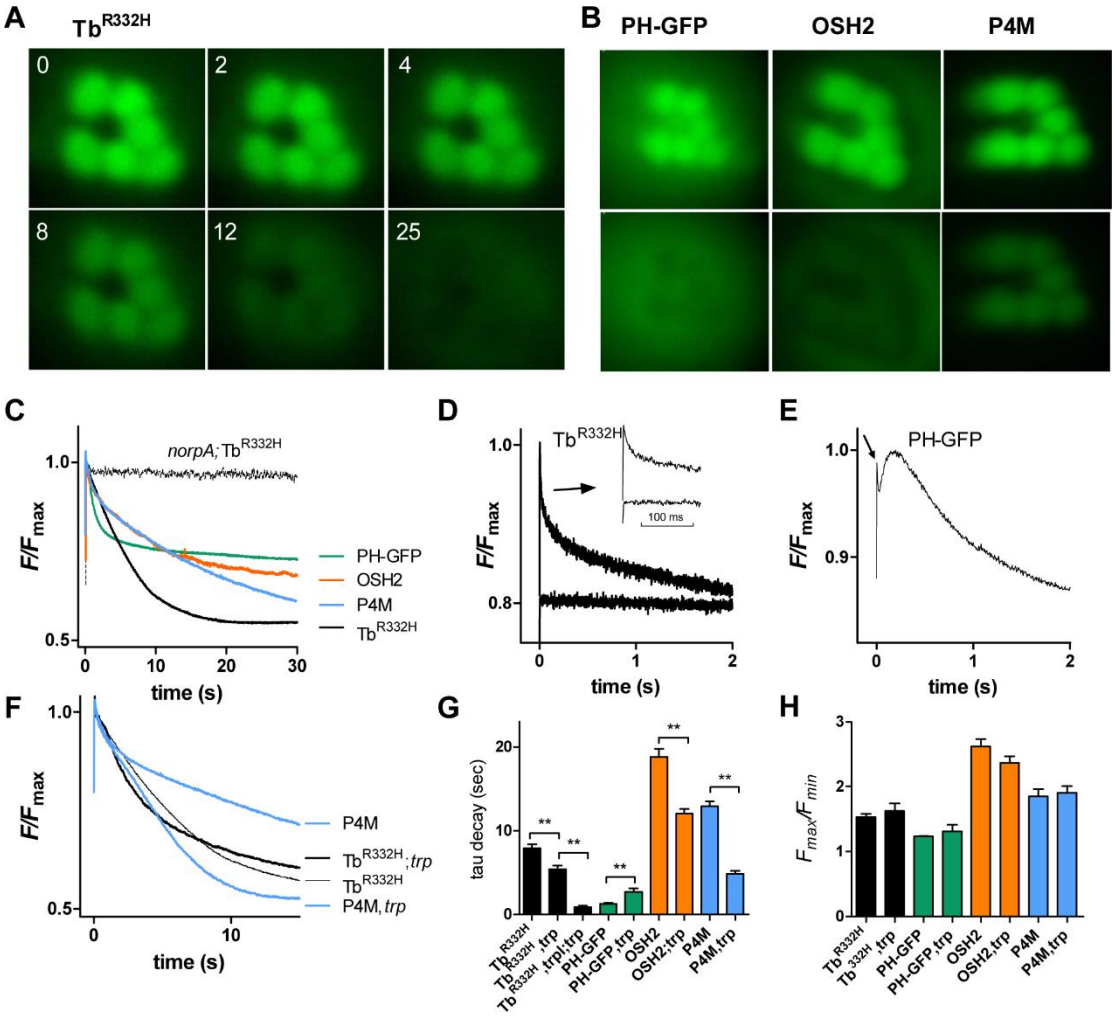

Figure 2 Time course of translocation from deep pseudopupil (DPP) of intact flies

(A) Images of DPP fluorescence in flies expressing Tb^{R332H} taken at 0,2,4,8,12 and 25 s after onset of blue excitation in an initially dark-adapted fly. **(B)** DPP fluorescence in flies expressing PH-GFP, OSH2 and P4M. Top image in each pair at t= 0; lower images taken 5 s (PH-GFP) or 60 s (OSH2 and P4M) later. Tb^{R332H}, OSH2, OSH1 and P4M were expressed under control of the Rh1 promoter, hence the central R7 rhbadomere appears as a dark hole lacking GFP; PH-GFP was expressed using the *trp* promoter and is also expressed in R7. **(C)** Representative PMT measurements of DPP fluorescence (sampled at 50 Hz from cropped regions (corresponding approximately to fields shown in A and B): each probe decayed (translocated) with a characteristic time course similar to that seen in dissociated ommatidia (c.f. Fig. 1B).

No translocation was detected in the null PLC mutant (*norpA*^{P24}). **(D)** Tb^{R332H} fluorescence on a rapid time scale (sampled at 500 Hz): an initial rapid transient (arrow, inset on faster timebase) reflects M to R photoisomerization by the blue excitation and was not seen if M was not first reconverted to R by orange/red light (lower traces). (**E**) PH-GFP fluorescence on a rapid timescale: after the R>M transient (arrow), fluorescence increased briefly (~200 ms) before decaying. (**F**) Traces of fluorescence decay of P4M and Tb^{R332H} on wild-type (same traces as in **C,** note different timescale) and *trp* mutant backgrounds. (**G**) Time constants (single exponential fits) of fluorescent decay traces in wild-type and *trp* backgrounds (mean ± s.e.m. n = 6-13). Decay was significantly ($P < 0.005$) faster in *trp* mutants for OSH2, P4M and Tb^{R332H}, but slower for PH-GFP. Decay for Tb^{R332H} was faster still (0.87 s) on the *trpl*;*trp* background. (**H**) Extent of translocation (F_{max}/F_{min} ratio) for each probe was similar on wt and *trp* backgrounds (mean ± s.e.m. n= 5-12). Note that comparisons of F_{max}/F_{min} between probes are not reliable because each transgene confers a different eye colour, which influences F_{max}/F_{min} (see methods and Supplemental text). PH-GFP was expressed on *cn,bw* (white-eyed) background (hence low F_{max}/F_{min} values); eye colour of others were various shades of orange.

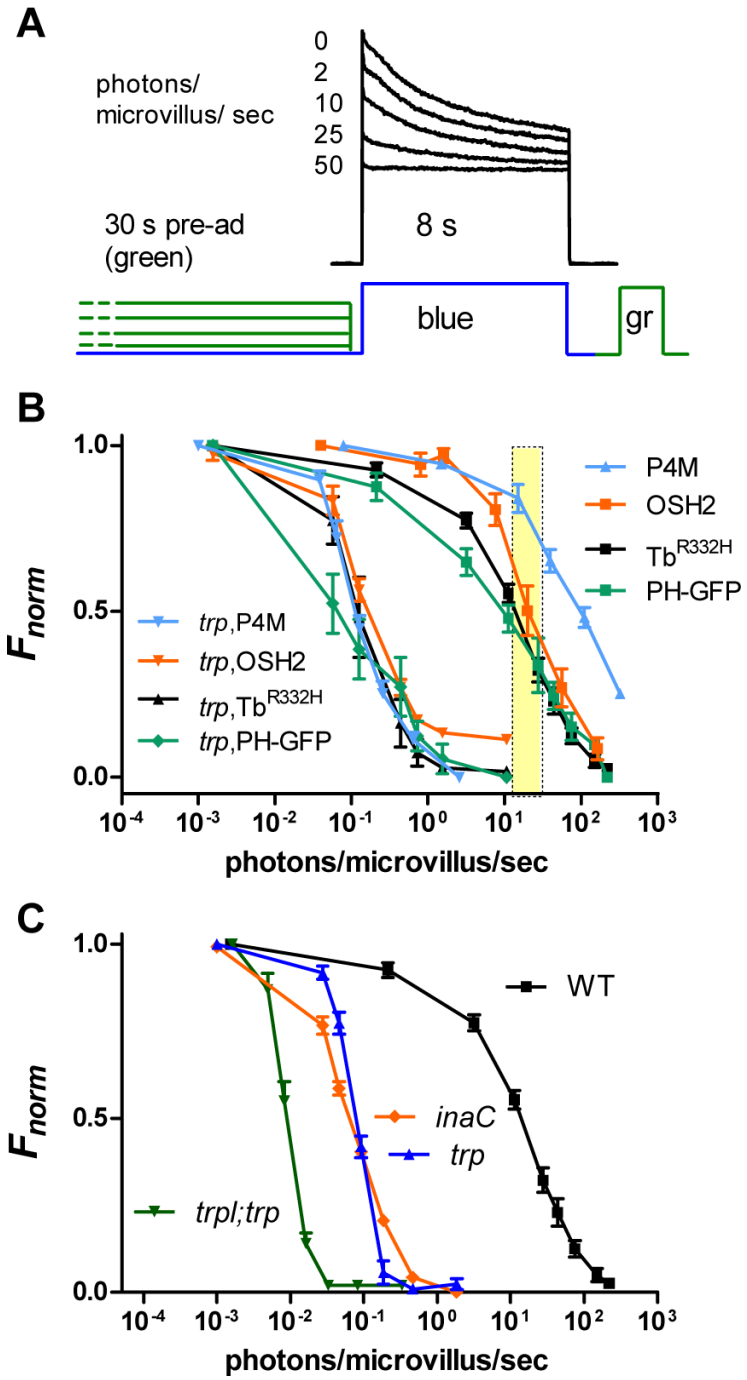

Figure 3 Intensity dependence of phosphoinositide depletion

(A) Tb^{R332H} fluorescence from DPP of intact fly. The fly was pre-adapted with varying intensities of long wavelength (green, 545 ± 50 nm) light for 30 s before measuring instantaneous fluorescence with blue excitation. M was then reconverted to R by photoequilibrating green (gr) illumination, and the fly dark-adapted for 2 minutes before the next measurement. **(B)** Fluorescence (normalized between F_{max} and F_{min}) as a function of intensity of the pre-adapting light expressed in effectively

absorbed photons/microvillus/second. On wild-type background, the PtdIns4*P* binding probes (OSH2 and P4M) required up to ~10x brighter illumination for effective translocation. PH-GFP showed significant depletion at slightly lower intensities than Tb^{R332H}. In *trp* mutants, PtdIns(4,5)P_2 and PtdIns4*P* were depleted with ~ 100x dimmer illumination (mean ± s.e.m. n = 6-10). The yellow bar represents estimate of brightest natural light levels (~0.5-1 x 10^6 photons/ photoreceptor/sec). (**C**) Tb^{332H} fluorescence as function of pre-adapting intensity in wild-type (replotted from **B**), trp^{343} (n = 15; independent data set from panel **B**), $inaC^{P209}$ (n = 21) and *trpl;trp* (n = 9).

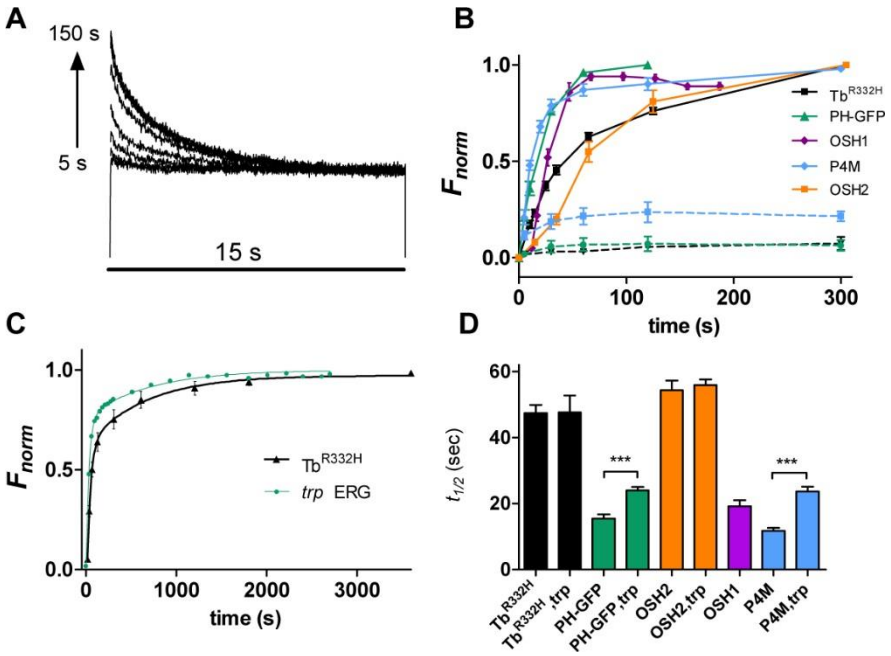

Figure 4 Time course of phosphoinositide resynthesis

(A) Superimposed series of fluorescence traces measured from DPP of a fly expressing Tb^{R332H}. Before each trace M was reconverted to R with photoequilibrating long wavelength illumination and then left in the dark for varying durations (5 – 150 s). Fluorescence recovered progressively, reflecting return of the PtdIns(4,5)P_2-specific Tb^{R332H} probe to the rhabdomeres and then decayed again during the 15 s blue excitation light. (**B**) Averaged, normalised (between F_{max} and F_{min}) recovery time courses for 5 different probes (mean ± s.e.m. n = 6-12 flies). Dotted lines: Tb^{R332H}, PH-GFP and P4M measured without first photoreisomerising M to R showed little or no recovery. (**C**) On a longer time scale, Tb^{R332H} showed a slow component of recovery taking up to ~1 hour to fully recover; a similar slow component was seen in the recovery of the ERG response in *trp*. Data fitted with two exponential fits (Tb^{R332H} 38 s, and 642 s; *trp* ERG 35 s and 776 s: mean ± s.e.m. n = 4). (**D**) half times ($t_{1/2}$) for recovery of fluorescence (to 50% of value after 5 minutes dark adaptation) were significantly slower on *trp* backgrounds for PH-GFP and P4M ($P < 0.001$), but not for Tb^{R332H} or OSH2. Mean ± s.e.m. (n = 7-10 flies).

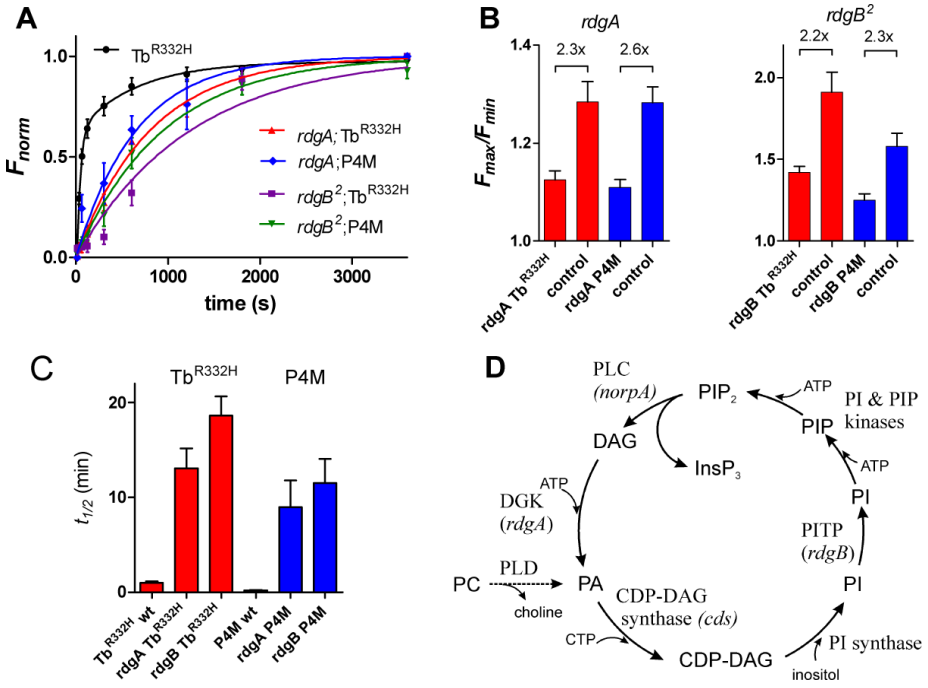

Figure 5 Phosphoinositide resynthesis in *rdgB* and *rdgA* mutants

(A) Normalised recovery of DPP fluorescence in flies expressing P4M and Tb^{R332H} following PtdIns(4,5)P_2 depletion in wild-type (Tb^{R332H} only, replotted from Fig. 4), *rdgB*^{2} and *rdgA*^{1}*;;trp*^{343} mutant backgrounds. PtdIns(4,5)P_2 and PtdIns4*P* resynthesis were greatly slowed in both *rdgA* and *rdgB*, but still recovered over ~1 hour. Mean ± s.e.m. n = 4-6: data fitted with exponentials (*rdgA;Tb* 805s; *rdgA;P4M* 650s, *rdgB;P4M* 950s; *rdgB;T*b 1250 s). **(B)** F_{max}/F_{min} ratios in *rdgA*^{1}*;;trp* and *rdgB*^{2} compared to eye-colour matched wild-type or *trp* controls expressing the same transgenes: the fold-reduction in F_{max}/F_{min} (indicated above each pair) provides an estimate of the reduction in maximum (dark-adapted) PtdIns(4,5)P_2 and PtdIns4*P* levels. **(C)** Half times (t ½) for recovery of Tb^{R332H} and P4M in *rdgA*^{1}*;;trp*^{343} and *rdgB*^{2} and wild-type controls (mean ± s.e.m n= 4-8). **(D)** Proposed phosphoinositide cycle in *Drosophila* photoreceptors. Note that phosphatidic acid (PA) could in principle also be generated from phosphatidyl choline (PC) by phospholipase D (PLD).

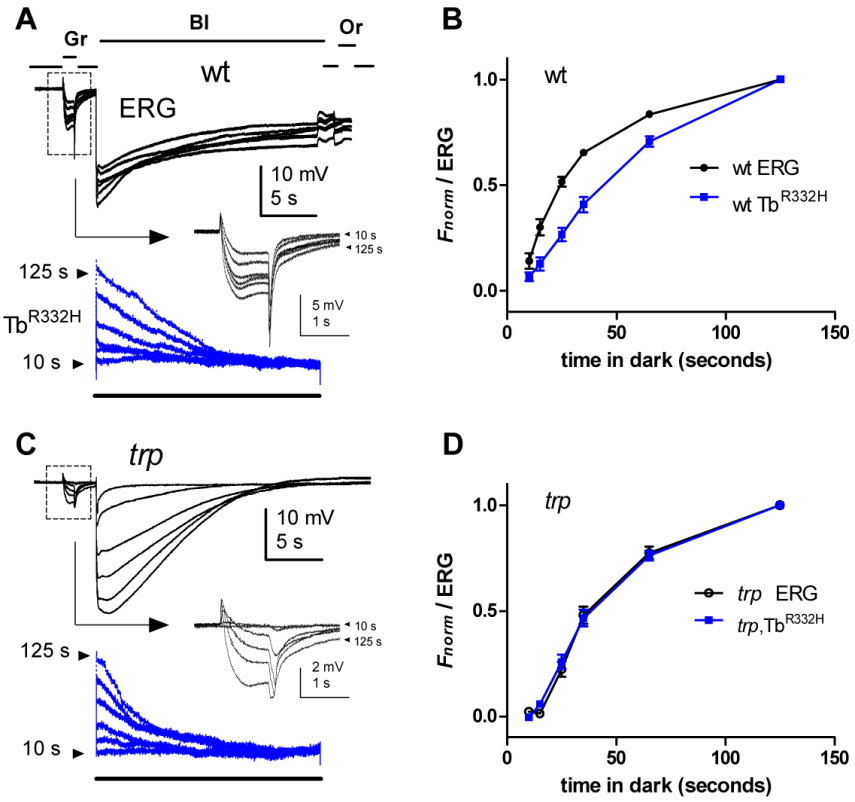

Figure 6 Simultaneous recordings of recovery from Tb^{R332H} and ERG.

(A) A 1 s green (Gr) test flash to test sensitivity in the ERG (top traces) was delivered prior to blue (Bl) illumination for 20s to excite Tb^{R332H} fluorescence (lower, blue traces): arrow points to responses to test flash (boxed) on expanded scale. Finally, an intense orange (Or) flash was delivered to reconvert M to R. The period in the dark between each sequence was varied from 10 - 120 s. In both wildtype **(A,B)** and *trp* **(C,D)** backgrounds, PtdIns(4,5)P_2 (Tb^{R332H} signal) was depleted by the blue excitation and resynthesised with a similar time course. **(B)** On the wt background, the normalised ERG response amplitude to the green test flash recovered significantly more quickly than Tb^{R332H} fluorescence (normalised between F_{max} and F_{min}); **(D)** whilst on the *trp* background the normalised ERG recovered with an almost identical time course. Plots in **B** and **D** are normalised mean data ± s.e.m., n = 10 (wt) or 7 (*trp*).

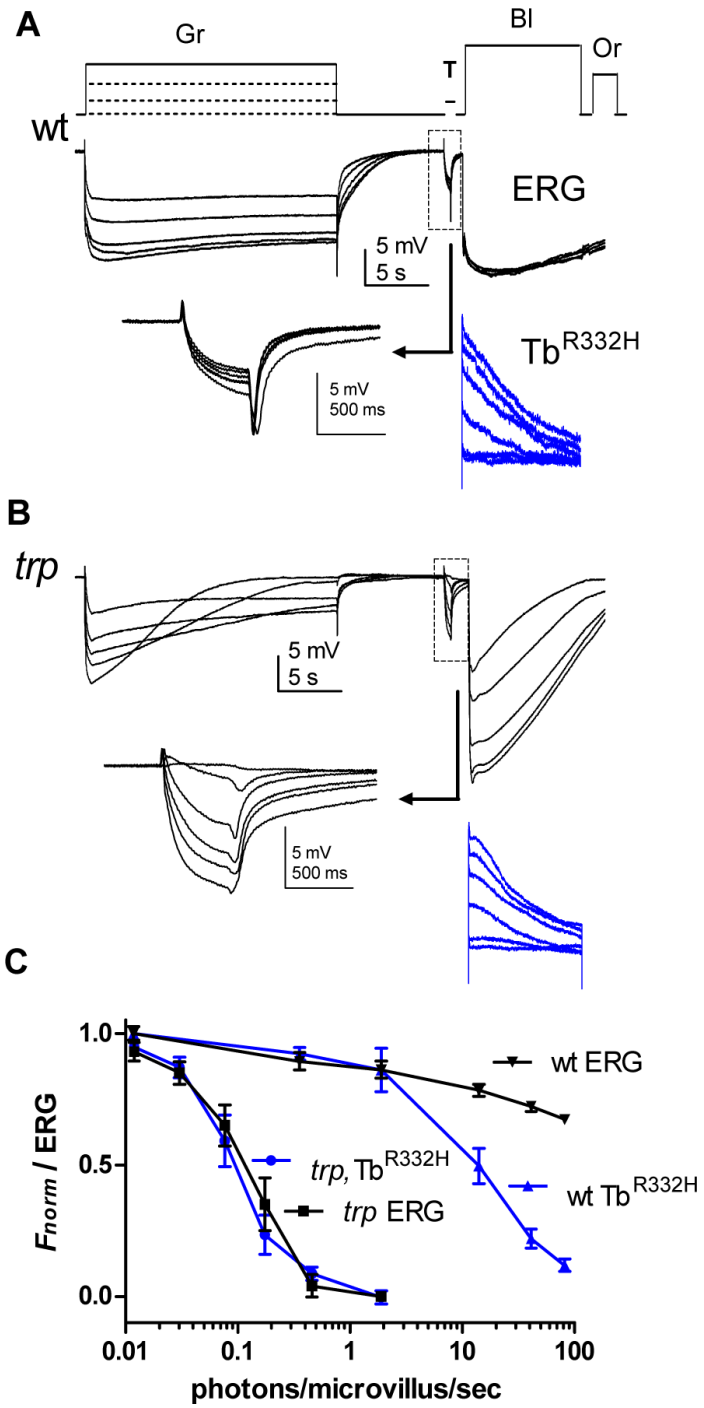

Figure 7 Simultaneous ERG and Tb^{R332H} measurements of the intensity dependence of PtdIns(4,5)*P*$_2$ depletion.

(A) Intact wild-type fly expressing Tb^{R332H} was first exposed to 25 s pre-adapting green (Gr) illumination of varying intensities, and sensitivity tested with a brief (500 ms) test flash (T, boxed region: arrow points to test response on expanded scale) immediately before measuring instantaneous fluorescence with blue (Bl) excitation

(Tb^{R332H}, blue traces). Orange (Or) light then reconverted M to R, and the flies were dark-adapted for 2 minutes before repeating with the next pre-adapting intensity. **(B)** Similar protocol in a *trp* mutant, using ~100x dimmer pre-adapting regimes (note *trp* decay at higher intensities). **(C)** Averaged, normalised data (mean ± s.e.m. n=7) comparing ERG test flash and Tb^{R332H} fluorescence as a function of pre-adapting intensity. In *trp* mutants, Tb^{R332H} and ERG data essentially overlap. On wild-type background, ERG sensitivity was only slightly reduced even after the brightest pre-adapting light (equivalent to ~100 effective photons/microvillus/sec), which had depleted ~ 90% of the PtdIns(4,5)P_2.

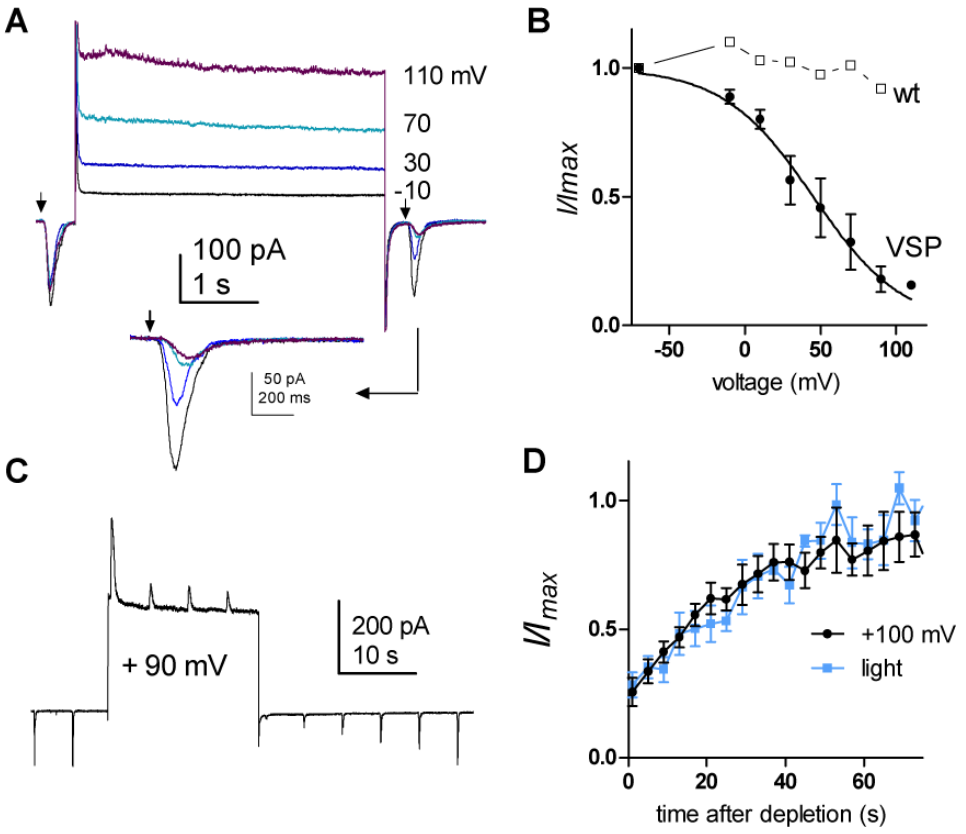

Figure 8 Depletion of PtdIns(4,5)P_2 by *Ciona* voltage-sensitive phosphatase (CiVSP)

(A) Whole cell recording from photoreceptor expressing CiVSP in presence of 100 µM La^{3+} to isolate TRPL current: following a brief test flash (arrow) 4 s voltage steps (-10 to +110 mV from holding potential of -70mV) were applied and sensitivity retested with a second test flash immediately on return to -70 mV (inset below on expanded scale). **(B)** Response of second test flash normalised to control prior to voltage step (I/I_{max}) as a function of voltage. Data fitted with a Boltzmann distribution, V_{50} +45 mV (mean ± s.e.m. n = 4). Similar data from a control wild-type cell (wt) showed no suppression. **(C)** Continuous recording showing responses to light flashes suppressed during a +90 mV voltage step (currents now outward), recovering over a period of ~30 s on return to -70 mV. **(D)** Averaged recovery time course data (normalised to test flash prior to voltage step ending at time zero, mean ± s.e.m. n = 7), compared to recovery time course of the light response following PtdIns(4,5)P_2 depletion by light stimuli calibrated to result in the same initial suppression in the same cells.